Volume 47, Number 3, 2021.

# Mobility & Vehicle Mechanics

*International Journal for Vehicle Mechanics, Engines and Transportation Systems*

ISSN 1450 - 5304

UDC 621 + 629(05)=802.0


| | | |
|---|---|---|
| Victor I. Popov, Lev M. Monosov, Igor V. Polischuk | ENVIRONMENTAL PROBLEMS AND THEIR SOLUTION DURING CONSTRUCTION AND OPERATION OF ST. PETERSBURG BARRIER FLOOD PROTECTION | 1-8 |
| Onur Güler, Sandra Gajevic, Slavica Miladinovic, Hamdullah Çuvalcý, Blaža Stojanovic | OPTIMIZATION OF ZINC-BASED HYBRID NANOCOMPOSITES USING TAGUCHI GREY RELATION ANALYSIS | 9-22 |
| Predrag Mrdja, Nenad Miljic, Slobodan Popovic, Marko Kitanovic | STATIONARY TEST PLAN OPTIMISATION USING SLOW DYNAMIC SLOPE ENGINE SCREENING | 23-33 |
| Luka Ponorac, Aleksandar Grkic, Slavko Muždeka | HYBRID POWER TRAINS FOR HIGH-SPEED TRACKED VEHICLES | 35-48 |
| Valentina Golubovic-Bugarski, Snežana Petkovic, Gordana Globocki-Lakic | THE EFFECT OF CORROSION ON A STRUCTURAL INTEGRITY AND VEHICLE SAFETY | 49-62 |


UNIVERSITY OF KRAGUJEVAC, FACULTY OF ENGINEERING

SERBIAN SOCIETY OF AUTOMOTIVE ENGINEERS

# M V M **M**obility **V**ehicle **M**echanics

*Editors: Prof. dr **Jovanka Lukić**; Prof. dr **Čedomir Duboka***

**MVM** *Editorial Board*
*University of Kragujevac*
*Faculty of Engineering*
*Sestre Janjić 6, 34000 Kragujevac, Serbia*
*Tel.: +381/34/335990; Fax: + 381/34/333192*



*For Publisher: Prof. dr Dobrica Milovanović, dean, University of Kragujevac, Faculty of Engineering*

***Publishing of this Journal is financially supported from:***
***Ministry of Education, Science and Technological Development, Republic Serbia***

**M**obility & **V**ehicle **M**echanics

**M**otorna **V**ozila i **M**otori

**Volume 47**
**Number 3**
**2021.**

| | | |
|---|---|---|
| Victor I. Popov, Lev M. Monosov, Igor V. Polischuk | ENVIRONMENTAL PROBLEMS AND THEIR SOLUTION DURING CONSTRUCTION AND OPERATION OF ST. PETERSBURG BARRIER FLOOD PROTECTION | 1-8 |
| Onur Güler, Sandra Gajević, Slavica Miladinović, Hamdullah Çuvalcı, Blaža Stojanović | OPTIMIZATION OF ZINC-BASED HYBRID NANOCOMPOSITES USING TAGUCHI GREY RELATION ANALYSIS | 9-22 |
| Predrag Mrđa, Nenad Miljić, Slobodan Popović, Marko Kitanović | STATIONARY TEST PLAN OPTIMISATION USING SLOW DYNAMIC SLOPE ENGINE SCREENING | 23-34 |
| Luka Ponorac, Aleksandar Grkić, Slavko Muždeka | HYBRID POWER TRAINS FOR HIGH-SPEED TRACKED VEHICLES | 35-48 |
| Valentina Golubović-Bugarski, Snežana Petković, Gordana Globočki-Lakić | THE EFFECT OF CORROSION ON A STRUCTURAL INTEGRITY AND VEHICLE SAFETY | 49-62 |

**M**obility & **V**ehicle **M**echanics

**Volume 47**
**Number 3**
**2021.**

**M**otorna **V**ozila i **M**otori

| | | |
|---|---|---|
| Victor I. Popov, Lev M. Monosov, Igor V. Polischuk | PROBLEMI ŽIVOTNE SREDINE I NJIHOVO REŠENJE TOKOM IZGRADNJE I RADA BARIJERE ZA ZAŠTITU OD POPLAVA SANKT-PETERBURGA | 1-8 |
| Onur Güler, Sandra Gajević, Slavica Miladinović, Hamdullah Çuvalcı, Blaža Stojanović | OPTIMIZACIJA HIBRIDNIH NANOKOMPOZITA BAZIRANIH NA CINKU PRIMENOM TAGUČI GREJ ANALIZE | 9-22 |
| Predrag Mrđa, Nenad Miljić, Slobodan Popović, Marko Kitanović | STACIONARNI TEST PLAN OPTIMIZACIJE PRAĆENJA KARAKTERISTIKE OPTEREĆENJA MOTORA SA MALIM KONSTANTNIM GRADIJENTOM PORASTA OPTEREĆENJA MOTORA | 23-34 |
| Luka Ponorac, Aleksandar Grkić, Slavko Muždeka | HIBRIDNI SISTEM POGONA ZA BRZOHODA GUSENIČNA VOZILA | 35-48 |
| Valentina Golubović-Bugarski, Snežana Petković, Gordana Globočki-Lakić | UTICAJ KOROZIJE NA INTEGRITET STRUKTURE I SIGURNOST VOZILA | 49-62 |

**MOBILITY & VEHICLE MECHANICS**

DOI: 10.24874/mvm.2021.47.03.01
**UDC: 627.51:502**

# ENVIRONMENTAL PROBLEMS AND THEIR SOLUTION DURING CONSTRUCTION AND OPERATION OF ST. PETERSBURG BARRIER FLOOD PROTECTION

*Victor I. Popov[1]*, Lev M. Monosov[2], Igor V. Polischuk[3]*

*Received in July 2020* *Revised in August 2020* *Accepted in September 2020*

RESEARCH ARTICLE

**ABSTRACT:** The report concerns the problems of ecology in the Eastern part of the Gulf of Finland and the Neva Bay during the construction and operation of St. Petersburg Barrie Flood Protection (KZS). The Barrier of Flood Protection includes 11 stone-earth dams, 2 ship-pass and 6 water-pass, a bridge with a lifting span of 102 m long and an underwater road tunnel with a length of about 2 km. The developed KZS project provides free water exchange, which has a minimal impact on the hydraulic regime and ecology of the water area of the Neva Bay. The protective structures fully implemented a systematic approach to collect, divert and clean up the entire volume of polluted water from the marine section of the ring road around St. Petersburg. KZS does not have a negative impact on the sanitary regime of the Neva Bay, on the reproduction of fish stocks, including valuable fish species. Moreover, protective structures play a huge role in preserving biodiversity and rare species of near-water and waterfowl.

**KEY WORDS**: flood, barrier of flood protection, ecology, dams



[1]*Victor I. Popov, PhD., Moscow State Motor and Road Technical University (MADI), Leningradsky prospect, 64, Moscow, Russia, vpopov@stpr.ru (*Corresponding author)*
[2]*Lev M. Monosov, PhD., Directorate of St. Petersburg Barrier Flood Protection (KZS), Torzkovskay str.5, St.Petersburg, Russia, lev_monosov@inbox.ru*
[3]*Igor V. Polischuk, Eng., Directorate of St. Petersburg Barrier Flood Protection (KZS), Torzkovskay str.5, St.Petersburg,Russia, ipol@fkpkzs.ru*

## PROBLEMI ŽIVOTNE SREDINE I NJIHOVO REŠENJE TOKOM IZGRADNJE I RADA BARIJERE ZA ZAŠTITU OD POPLAVA SANKT-PETERBURGA

**REZIME**: U radu se analizira probleme ekologije u istočnom delu Finskog zaliva i Nevskog zaliva tokom izgradnje i rada barijere za zaštitu od poplava Sankt Peterburga (KZS). Barijera za zaštitu od poplava obuhvata 11 brana od kamene i zemlje, 2 brodska i 6 rečnih prelaza, pokretni most dužine 102 m i podvodni tunel dužine oko 2 km. Razvijeni projekat KZS obezbeđuje slobodan tok vode, što ima minimalan uticaj na hidraulični režim i ekologiju vodotokova Nevskog zaliva. Zaštitne konstrukcije su u potpunosti primenile sistematski pristup prikupljanja, preusmeravanja i čišćenju celokupne količine zagađene vode sa morske deonice obilaznice oko St. Peterburga. KZS nema negativan uticaj na sanitarni režim Nevskog zaliva, na reprodukciju ribljeg fonda, uključujući vredne vrste riba. Štaviše, zaštitne strukture igraju ogromnu ulogu u očuvanju biodiverziteta i retkih vrsta ptica.

**KLJUČNE REČI**: poplava, barijera zaštite od poplava, ekologija, brane

# ENVIRONMENTAL PROBLEMS AND THEIR SOLUTION DURING CONSTRUCTION AND OPERATION OF ST. PETERSBURG BARRIER FLOOD PROTECTION

*Victor I. Popov, Lev M. Monosov, Igor V. Polischuk*

## INTRODUCTION

In 2020, nine years have passed since the commissioning of St. Petersburg Barrier of Flood Protection (KZS). The KZS is an extended marine hydraulic structure built in the freezing Gulf of Finland. Its length is more than 25 km, with 17.5 km passing through the open water area of the Eastern part of the Gulf of Finland. High-speed road on the11 stone and earthen dams, 6 culverts, 2 navigation structures C-1 and C-2 spans of 200 m and 116 m respectively, tunnel under navigation structure C-1 length 1961 m, steel bridge with lift span over the navigation structure C-2, the approach channels to the navigation structures C-1 and C-2, office of the KZS on the island Kotlin with the Central panel of the flood warning system KZS are included (Figure 1). During the 317 years of St. Petersburg's existence, there have been more than 300 rises in the water level above the 160 cm mark of the Baltic system, which considered as floods. Among them are three disastrous ones in 1777.1824 and 1924 .The most exceptional flood in height (H = 421 m) occurred on November 19, 1824 and was called the "flood". Two-thirds of the city's territory was flooded and more than 20 people was killed of this flood. The Flood of 1924 stimulated the development of a project to protect Leningrad from floods (Figure 2). In 1972-1976 years by the Institute Lengidroproekt was developed technical project of KZS. 52 design and survey and research institutes of the USSR took part in its creation. The project by the State expertise and by the government of the USSR in December 1978. In 1979, the construction of the protective complex began was approved.

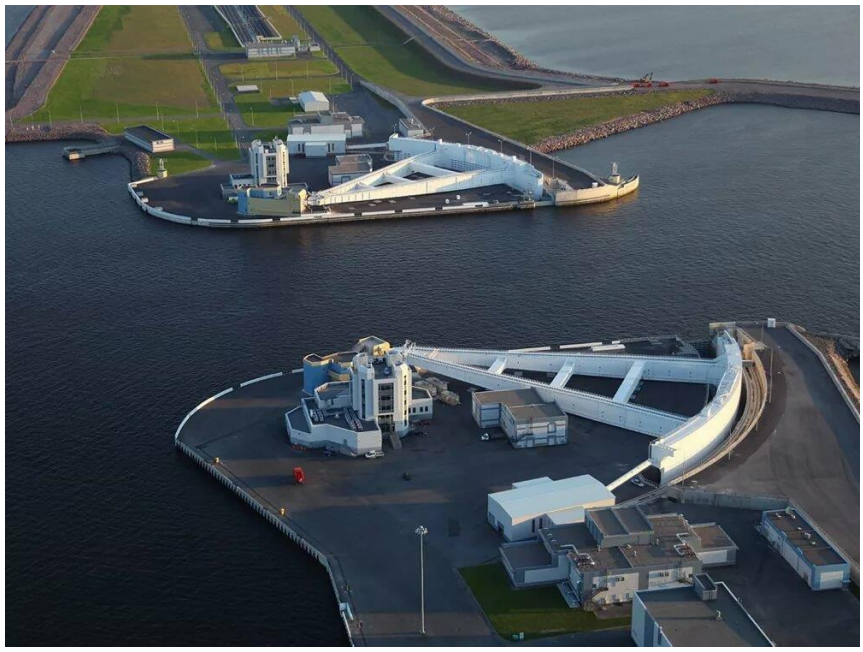

*Figure 1 Navigation structures C-1*

*Figure 2 Typical flood in St. Petersburg*

At this time, a number of well-known experts claimed that the construction of protective structures led to a violation of the hydrodynamic, hydrochemical and hydrobiological relationship of the Finland Gulf and the Neva Bay. At the same time, they attributed the deterioration of the sanitary condition of the Neva Bay to the construction of protective structures, and not to a sharp increase in concentrated discharges into the Northern channels of the Neva river Delta from centralized treatment facilities. However the Neva Bay is merged with the Finland Gulf by two Straits: the Northern and Southern gates, which have extensive shoals that prevent the penetration of sea wind waves and wind currents into the Neva Bay, the removal of ice from the Bay To the Gulf, and hinder water exchange between fresh and brackish waters of the Bay. Therefore, the Neva Bay is essentially a closed basin, which has always formed a local hydrological regime, little affected by the Gulf of Finland. Some experts believed that floods contribute to the purification of the Neva Bay and the Delta of the Neva. As shown numerous field tests a result of intensive cyclonic activity during floods in the Eastern part of the Finland Gulf there has always been a mixing of waters and a retreat to the West of the wedge of brackish water (from 30 to 90 km) from the target of protective structures and therefore their statements should be considered incorrect. The design solutions implemented correctly during the construction process did not change the system of currents, wave and temperature regimes, or the natural regime of water levels in the Neva Bay and the Delta of the river. Neva. As in everyday life, the project provided levels well below the ordinary (Figure 3).

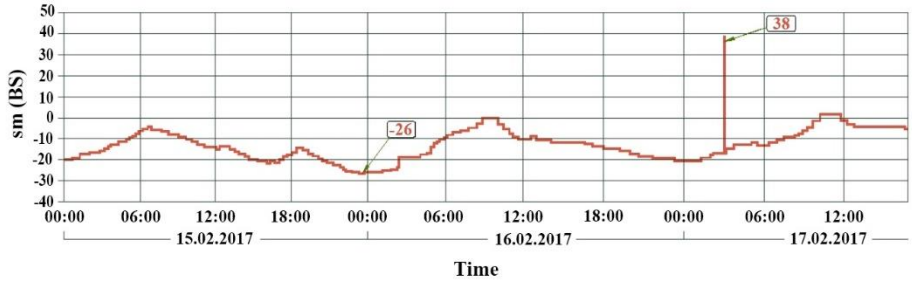


*Figure 3 Water Level below the ordinary on the date of 15.02.2017.*

Insufficiently justified public statements of well-known experts provoked in the late 80-ies of the last century in the society an acute discussion on the problems of environmental safety of the complex of protective structures under construction. As a result, in October 1990, the Leningrad authorities decided to suspend the construction of the KZS.

## 1. ENVIRONMENTAL ASPECTS OF THE KZS PROJECT

In 2004, the Russian Government entered into a loan agreement with the EBRD to finance the completion of the KZS. Considering that the project has not been conserved for 14 years, the unfinished objects have actually become a source of environmental pollution of the Neva Bay. Leading Russian specialists, as well as foreign experts from the UK (Halkrou) and the Netherlands (Roal Haskoning) were involved in the development of the project documentation for the completion of the KZS. The completion project contained a section on the environmental justification of the facility (environmental Protection). The construction of the barrier began in 2006. 6 contracts were concluded on the basis of standard FIDIC contracts (red and yellow books). Since the beginning of the construction of the KZS, the problem of pollution was gradually decrease and contribute to this the conditions created for the completion of the construction of KZS facilities. During the operation of the Complex, as well as during the construction period, environmental issues were also much attention was paid [1]. The required quality of environmental safety was also monitored by environmental experts from the EBRD occasionally visited the facility under construction. Also constant supervision was provided for the government Agency for technological and environmental monitoring (Rostekhnadzor of Russia). In 2010, the KZS Directorate issued decisions on granting a water body for use, which defined a safety zone, including an environmental zone in the Baltic sea. The total area of this zone, for which the KZS Directorate is responsible, is 21 square km. The main threat to the adjacent water basin during the operation of the KZS is surface water runoff (diffusive runoff) from the roadway of the marine section of the ring road. On this section of 25.4 km long, the six-lane highway is capable of passing up to 27,500 vehicles per day at an estimated speed of 120 km/h. Taking into account the high and increasing traffic intensity along the highway every year, a systematic approach was developed and implemented to collect, divert and clean up the entire volume of polluted water. These large-scale measures made it possible to prevent the discharge of untreated sewage into the water area. The complexity of the organizing task for collection and treatment of effluents from the entire KZS was associated with extremely limited areas of dams and the presence of six bridges on the route at the culverts and at the C-2 ship-passing structure of the drawbridge and a deep-water road tunnel (Fig.4) [1, 2]. System of drainage pipes and trays placed above the bridge are intended for clean the diffusion runoff from the roadway of bridges over culverts. Water supplied for cleaning in

special combined filter cartridges filled with clinoptilolite (a mineral from the Kholinsky Deposit of Buryatia) and activated carbon. 118 such filter cartridges are installed on the bridge supports.

*Figure 4 Drawbridge with ship-passing structure C-2*

To treat wastewater entering a deep-water road tunnel, a water removal system is used, which consists of water-collecting drainage trays, receptacles of receiving tanks for collection and pumping, three pumping stations, and treatment facilities. The main pollutants present in the surface runoff of the tunnel are mineral and organic impurities of natural origin, substances of natural origin in various phase-dispersed States, petroleum products, washed - out components of road surfaces, heavy metal compounds, surfactants (synthetic surfactants), bacterial contamination. A mandatory element of surface treatment facilities is an accumulating sump. Treatment facilities of the road tunnel S-1 KZS provide for physical and chemical treatment of surface runoff after the accumulating sump. The coagulation process with subsequent water filtration allowed to obtain purified water at the outlet with the indicators established by the standards for fish and farm reservoirs. Discharge of treated water from treatment facilities to the water area is made if its composition meets the regulatory requirements for suspended substances, biochemical oxygen consumption, chlorides and petroleum products. Sufficient to say, that all local treatment facilities used at the KZS produced in Saint Petersburg. They are resistant to low temperatures and corrosion. It can be stated, that at present the KZS Directorate has implemented a plan of water protection measures in accordance with the requirements of the Water code and the Water strategy of Russia for the period up to 2025. For the first time in Europe, 100% treatment of surface runoff from the long sea section of the KZS highway has been provided, and water enters the Baltic sea only after it has been cleared of pollution. These measures are an important part of the Russian party's implementation of the Convention for the protection of the marine environment of the Baltic sea area (Helsinki Convention) and its recommendations to reduce discharges from urban areas by properly regulating the stormwater system. The operated complex of structures to protect Saint Petersburg from flooding does not adversely affect the sanitary regime of the Neva Bay, on the reproduction of fish stocks, including valuable passing and semi-passing fish. The

process of sustainable restoration of the ecosystem in the KZS zone after the completion of the construction period has been stable. This evidence that is preservation of living conditions for almost 60 species of aquatic and near-water birds that migrate annually through the Gulf of Finland (Figure 5) [3, 4]. In the areas immediately adjacent to the protective structures, there is an annual appearance in the spring of white and black swans, Curlews, capercaillie, terns and other birds listed in the Red book, as well as the appearance of predatory mammals - red foxes and weasels. A permanent approach to ship and culvert structures of the seal KZS (Pinipedia) is noted (Figure 6).

*Figure 5 Swans in the Gulf of Finland*

*Figure 6 Red fox and seal*

For the first time after the completion of construction, in May 2016, a large number of very rare plants listed in the Red book – Primula (Primula) - were grown on the lawns of the KZS.

## 2. CONCLUSIONS

1. The commissioning of the KZS in 2011 and the completion of the main sewer collector in the Northern part of the city were the main factors contributing to the purification of the Neva Bay and the Neva river Delta. Currently industrial and municipal water discharges in the Neva river are 100 purified%.
2. At present, the Neva Bay is separated from the Gulf of Finland by protective structures of exceptional environmental significance. Culverts with a total living area of 9540 m2 and a spillway front of 1864 m, which is 1.5 times larger than the mouth of the Neva river.
3. KZS gates are always open in their normal state, providing full "transparency" for the free movement of water and biota between the Gulf of Finland and the Neva Bay. The system of currents, wave and temperature regimes, the natural regime of water levels in the Neva Bay and the Delta of the river. The Neva river has not changed. As in everyday life, there are constantly marked levels well below the ordinary. Flooding of the city does not occur.
4. If there is a threat of flooding, all ship and culvert structures of the protective complex cover the Neva Bay, and it turns into a closed water area. The closed gates of the KZS prevent the transfer of a huge amount of bottom sediments from the Eastern part of the Gulf of Finland to the Neva Bay by drift currents. Therefore, there is no pollution of the Neva Bay from the Gulf of Finland. In the Neva Bay itself, during this period, there is an accumulation of runoff of the Neva river.
5. After the flood situation ends, levels are leveled and all gates of protective structures are opened, when the level drops, the Neva river, unlike the living conditions, no longer carries water with a high concentration of pollutants into the Neva Bay.
6. Implemented design solutions have created favorable conditions for the successful recovery of the ecosystem after entry to the GLC in operation.
7. Successful operation experience confirmed the conclusions of scientists, designers, and an International Commission of independent experts on the environmental safety of protective structures.
8. Experience of the KZS operation clearly shows that the environmental safety of the water area and adjacent territories contributed to the rapid restoration of the ecosystem after the completion of the KZS construction.

## REFERENCES

[1] Migurenko, V.: “Actual problems of Flood Protection Barrier maintenance”, Гидротехническое строительство, 2015, No. 8, pp. 56-58.

[2] Popov, V., Monosov, L.: “Technical supervision in the Project of Flood Protection Barrier completion”, Гидротехническое строительство, 2013, No. 5, pp. 18-22.

[3] Popov, V., Monosov, L.: “Five years operation main results of St. Petersburg Flood Protection Barrier”, Znanstvena misel journal, 2017, No. 4, pp. 126-133.

[4] Monosov, L., Popov, V.: “To environmental issues when summarizing the experience of designing, building and operating of Flood Protection Barrier in Saint Petersburg”, Materials of the IX International scientific and practical conference on June 10 2018, Yekaterinburg, pp. 36-46.

**MOBILITY & VEHICLE MECHANICS**

DOI: 10.24874/mvm.2021.47.03.02
**UDC: 66.018**

# OPTIMIZATION OF ZINC-BASED HYBRID NANOCOMPOSITES USING TAGUCHI GREY RELATION ANALYSIS

*Onur Güler[1]*, Sandra Gajević[2], Slavica Miladinović[3], Hamdullah Çuvalcı[4], Blaža Stojanović[5]*

*Received in July 2020* *Revised in August 2020* *Accepted in February 2021*

RESEARCH ARTICLE

**ABSTRACT:** Hybrid nanocomposites have wide application in many industries. Nanocomposites with base alloy ZA27 reinforced with $Al_2O_3$ and Gr are commonly used for bearing applications. Taguchi based Grey relational analysis (GRA) was applied for the multi response optimization of parameters of nanocomposite for improving the tribological characteristics. In this investigation considered parameters are load (10, 15, 20, 25 N), reinforcement content of Gr and $Al_2O_3$ (1, 2, 3, 4 vol.%), while time and speed are constant as 30 min and 100 rpm, respectively. ANOVA analysis was used to determine influence parameters on wear loss and coefficient of friction (CoF) of nanocomposite. It was observed that the most influential parameter on tribological characteristics of nanocomposites was reinforcement content of $Al_2O_3$. Combination of parameters for optimal tribological characteristics is A1B1C4 i.e. load of 10 N, reinforcement content of 1 vol.% Gr and reinforcement content of 4 vol.% $Al_2O_3$. Obtained nanocomposite has shown good tribological properties which lead to less wear loss and therefore expectedly longer life of the bearing in various segments of the automotive industry.

**KEY WORDS**: nanocomposite, optimization, wear loss, coefficient of friction, Taguchi Grey relational analysis



[1]*Onur Güler, Research assistant, Karadeniz Technical University, Department of Metallurgical and Materials Engineering, 61080, Trabzon, Turkey, onurguler@ktu.edu.tr (*Corresponding author)*
[2]*Sandra Gajević, Teaching assistant, Faculty of Engineering University of Kragujevac, Department of Mechanical Constructions and Mechanization, Sestre Janjic 6, 34000 Kragujevac, Serbia, sandrav@kg.ac.rs*
[3]*Slavica Miladinović, Research assistant, Faculty of Engineering University of Kragujevac, Department of Mechanical Constructions and Mechanization, Sestre Janjic 6, 34000 Kragujevac, Serbia, slavicam@kg.ac.rs*
[4]*Hamdullah Çuvalcı, PhD prof., Karadeniz Technical University, Department of Metallurgical and Materials Engineering, 61080, Trabzon, Turkey, hcuvalci@ktu.edu.tr*
[5]*Blaža Stojanović, Associate prof., Faculty of Engineering University of Kragujevac, Department of Mechanical Constructions and Mechanization, Sestre Janjic 6, 34000 Kragujevac, Serbia, blaza@kg.ac.rs*

## OPTIMIZACIJA HIBRIDNIH NANOKOMPOZITA BAZIRANIH NA CINKU KORIŠĆENJEM TAGUCHI SIVE ANALIZE

**REZIME**: Hibridni nanokompoziti imaju široku primenu u mnogim industrijama. Nanokompoziti sa baznom legurom ZA27 ojačani $Al_2O_3$ i Gr uobičajeno se koriste kod ležajeva. Grejeva relaciona analiza (GRA) zasnovana na Taguči metodi primenjena je za optimizaciju parametara nanokompozita kako bi se poboljšale tribološke karakteristike. U ovom istraživanju razmatrani su parametri: opterećenje (10, 15, 20, 25 N), sadržaj ojačanja Gr i Al2O3 (1, 2, 3, 4 vol.%), dok su vreme 30 min i brzina 100 o/min bili konstantni. Analizom ANOVA utvrđeni su parametri koji deluju na smanjenje habanja i koeficijenta trenja (CoF) nanokompozita. Uočeno je da je najuticajniji parametar na tribološke karakteristike nanokompozita sadržaj ojačanja $Al_2O_3$. Kombinacija parametara za optimalne tribološke karakteristike je: A1B1C4, odnosno opterećenje od 10 N, sadržaj ojačanja 1 vol.% Gr i sadržaj ojačanja 4 vol.% $Al_2O_3$. Dobijeni nanokompozit pokazao je dobra tribološka svojstva koja dovode do manjeg habanja i stoga očekivano duži vek trajanja ležaja u različitim segmentima automobilske industrije.

**KLJUČNE REČI**: nanokompozit, optimizacija, smanjenje habanja, koeficijent trenja, Taguči Grej relaciona analiza

# OPTIMIZATION OF ZINC-BASED HYBRID NANOCOMPOSITES USING TAGUCHI GREY RELATION ANALYSIS

*Onur Güler, Sandra Gajević, Slavica Miladinović, Hamdullah Çuvalcı, Blaža Stojanović*

## INTRODUCTION

Successful and wide use of composite material has led to a development of a new field of research in engineering-nanocomposites. Nanocomposite is a material which consist of base material and reinforcement (particles, short and long fibers, tubes) whose one dimension is less than 100 nm. There are three types of nanocomposites, depending of the base material, and they are: Metal Matrix Nanocomposites (MMNC's), Polymer Matrix Nanocomposites (PMNC's) and Ceramic Matrix Nanocomposites (CMNC's). All of these nanocomposites have found their application in various industries, according to their mechanical and tribological characteristics. In automotive industry nanocomposites, especially with particle reinforcement, are applied for vehicles' body parts, chassis and tires, automotive interiors, electrical and electronics, and other [1]. Mostly used materials for base of composites are aluminium, magnesium, copper, zinc and titanium. Among various alloys used for MMC, zinc-based alloys are gaining wide spread popularity as a cost effective substitute. Zinc-based alloy ZA-27 has superior weight-to-strength ratio, as well as good corrosion and wear resistance. Because of their good tribological and mechanical properties these alloys are used for sliding bearings [2]. A lot of optimization methods are applied for increasing productivity, development and manufacturing of nanocomposites. In automotive industry there has been a great interest for use of optimization in aim of reduction of vehicle weight, costs of production and fuel consumption. Widely used optimization method is Taguchi analysis which is used for determination of the effects of all process parameters using a small number of experiments, but it is only applied for optimization of single response. In case of multi response optimization Taguchi is paired with Grey relation analysis (GRA). Investigation of tribological and mechanical characteristics of ZA27 composites on micro/nano scale was done by Babic et al. Nanocomposites with particle contents of 1, 3, and 5 vol.% SiC (mean size of 50 nm) were used as reinforcement and manufactured with the compocasting process. They concluded that wear resistance of nanocomposite improves with the increase of content of SiC nanoparticles in relation to base alloy. As for mechanical characteristics they concluded that with reduction of porosity micro/nano hardness increases. The highest porosity was for 1 vol.% SiC [3]. Influence of reinforcement on tribological characteristics of hybrid nanocomposite was investigated by Güler et al. They established that the lowest wear was for reinforcement content of 4 vol.% Gr and 4 vol.% Al2O3, and highest was for the base alloy. It was found that wear mechanism of nanocomposite was adhesion [4]. Pul et al. observed influence of nano reinforcement (0.5, 1.0, 2.0 and 4.0 wt.% Gr) and different sintering temperatures on tribological and mechanical characteristics of nanocomposite. By analysis of the results they concluded that with increase of content of nano reinforcement in ZA27 the porosity increased and mechanical strength decreased [5]. Taguchi method was applied by Kumar et al. for optimization of dry sliding wear performance of hybrid nanocomposite. Nanocomposites' consisted of ZA base alloy with ceramic reinforcement (1.5 wt.% SiC) and soft graphite (0.5 wt.% Gr) produced with ultrasonic assisted stir casting. With ANOVA analysis it was found that most influential parameter is distance and then with the use of S/N ratio optimal combination for minimum wear volume loss was established (sliding speed 1.5 m/s, load 40 N and sliding distance 500 m). Additionaly they found that hybrid composite showed better tribological properties in compare to base alloy [6]. Another use of Taguchi method for wear

optimization of ZA27/SiC nanocomposites was observed in research of Almomani et al. [7]. They applied Taguchi L16 orthogonal array with variation of following parameters SiC content (2, 3, and 4 wt.%), sliding speed (150 and 200 rpm) and load (40 and 75 N). Unlike conclusions made by Babic et al. [3] authors in this research found that with increase of SiC weight fraction, porosity content of MMNC's increased. By applying ANOVA analysis they observed that statistically significant parameters on wear rate are reinforcement contents and normal load. Based on SEM analysis wear mechanism of nanocomposite was abrasive wear. Stir casting fabricated nanocomposites with ZA alloy base and $Al_2O_3$ nanoparticles (1, 2 and 3 wt.%) were investigated by Shivakumar et al. [8]. It was noted that with increase of $Al_2O_3$ content microhardness increases and density of the nanocomposites decreases. Tribological testing and analysis of results was based on Taguchi orthogonal array L16. Optimal combination of parameters for minimum wear volume loss was as following: content of 3 wt.% $Al_2O_3$, sliding speed of 1 m/s, load of 30 N and sliding distance of 750 m. ANOVA analysis determined that the most significant parameter for minimum wear volume loss was sliding distance. Improvement of mechanical characteristics of ZA27 based nanocomposites compared to base alloy was presented by Bobić et al. [9]. Nanocomposites with nanoparticle reinforcement of $Al_2O_3$ (20–30 and 100 nm) and SiC (50 nm) were fabricated with mechanical milling and compocasting. Compared to base alloy improvements are shown in percents through hardness and yield strength [9]. Improvements of hardness of zinc-based nanocomposites are proven by Karimzadeh et al. in [10]. In their research they stated that microhardness of nanocomposites (350 HV) improved and was 10–15 times higher than that of the zinc based (20–30 HV). Based on literature review it can be observed that there is a small number of research and published results for tribological behaviour of ZA 27 based nanocomposites. Generally by observing the research of other composites' optimization methods were widely applied, as well as their combinations such as: ANN-Taguchi, RSM-Taguchi Grey and GA–ANN-PSO. A large variety of research was done with the use of statistical methods in the aim of establishing the relationship between optimal mixing proportion of material, tribological and mechanical properties, surface roughness, parameters of material processing, welding parameters, and others. Optimization of relationship between wear loss, coefficient of friction, load and reinforcement Gr and $Al_2O_3$ by Taguchi Grey method has not yet been investigated. This paper investigates tribological properties of ZA-27 nanocomposites using multi response optimization method for reduction of experiments' time and cost. Taguchi Grey performs multi response optimization by converting it to a single relational grade. Author Güler et al. in their research, concluded which composition of nanocomposites has the highest wear resistance but they didn't take into account both responses at the same time (CoF and wear loss). Purpose of this paper is to examine the parameters with the most significant effect on wear loss and CoF. By using Taguchi Grey analysis importance order of load, and reinforcement content of Gr and was determined and ANOVA analysis gave statistically significant parameters.

## 1. EXPERIMENTAL SETUP

### *1.1 Material*

ZA-27 alloy has been taken as base material for preparation of nanocomposites. The chemical composition of the ZA-27 base alloy consists of Al (25-28 wt.%), Cu (2.0-2.5 wt.%), Mg (0.01-0.02 wt.%) and Zn (balance). nanoparticles of $Al_2O_3$ and Gr have been selected as reinforcement material with average particle size of 50 nm and 100 nm, respectively. Mechanical milling process was used in the production of nanocomposite powders including 1-4 vol.% $Al_2O_3$ and Gr reinforcement particles and ZA27 base powders.

Mechanical milling operations were carried out in a planetary milling machine (Retsch PM 100) containing chamber and balls made of tungsten carbide. The rotation speed of 300 rpm, the ball: powder ratio of 5:1 and the milling time of 8 h were selected as milling parameters [11]. In order to prevent the sticking of ZA27 base powders having a ductile structure into the milling chamber walls during milling, 3% by weight of methanol was used as the process control agent (PCA). Firstly, nanocomposite powders produced by mechanical milling were cold pressed under a pressure of 175 MPa in a mold made of hot work steel. Later, nanocomposite samples were fabricated by hot pressing process with sintering of the cold-pressed samples in the mold for 4 h at 432 ºC and pressing them under 350 MPa to obtain the final nanocomposite samples. Tribometer with contact geometry block-on-ring is used to test the dry sliding wear behavior of ZA-27/$Al_2O_3$/Gr nanocomposites in which the observed response was the coefficient of friction and wear loss. The details about other production and wear tests were comprehensively indicated in the previous study [4].

### *1.2 Design of experiments*

A lot of statistical methods are used nowadays to observe the effect of controllable parameters on response, one of them is Taguchi method. This method uses orthogonal arrays in order to reduce experimental errors, number of experiments, time and cost, enhance the efficiency, optimize the process parameters and reproducibility of experiments. In this paper, three four-level factors, shown in Table 1, were considered in order to obtain the optimum combination for the nanocomposite with the lowest coefficient of friction and wear loss.

***Table 1*** *Name and level of parameters*

| Parameters | Units | Level I | Level II | Level III | Level IV |
|---|---|---|---|---|---|
| A: Load | N | 10 | 15 | 20 | 25 |
| B: Content of Gr | vol.% | 1 | 2 | 3 | 4 |
| C: Content of Al2O3 | vol.% | 1 | 2 | 3 | 4 |

Taguchi mixed L16 orthogonal array (Table 2) was obtained using MINITAB19 statistical software.

***Table 2*** *Experimental results and L16 orthogonal array*

| No.exp. | A | B | C | CoF | Wear loss (mg) |
|---|---|---|---|---|---|
| 1 | 10 | 1 | 1 | 0.343254 | 9.8 |
| 2 | 10 | 2 | 2 | 0.267246 | 9.0 |
| 3 | 10 | 3 | 3 | 0.335479 | 10.0 |
| 4 | 10 | 4 | 4 | 0.235487 | 6.2 |
| 5 | 15 | 1 | 2 | 0.325102 | 6.5 |

| | | | | | |
|---|---|---|---|---|---|
| 6 | 15 | 2 | 1 | 0.294563 | 16.6 |
| 7 | 15 | 3 | 4 | 0.299985 | 9.2 |
| 8 | 15 | 4 | 3 | 0.267863 | 12.1 |
| 9 | 20 | 1 | 3 | 0.262101 | 8.9 |
| 10 | 20 | 2 | 4 | 0.236892 | 10.4 |
| 11 | 20 | 3 | 1 | 0.387983 | 21.4 |
| 12 | 20 | 4 | 2 | 0.364786 | 26.3 |
| 13 | 25 | 1 | 4 | 0.235075 | 6.3 |
| 14 | 25 | 2 | 3 | 0.243154 | 8.8 |
| 15 | 25 | 3 | 2 | 0.379857 | 21.1 |
| 16 | 25 | 4 | 1 | 0.385413 | 30.2 |

### *1.3 ANOVA and Grey relation analysis (GRA)*

Within Taguchi method final step is identification of influence of each parameter on the response parameters using Analysis of Variance (ANOVA). ANOVA was performed with the assumption of 95% confidence level to get the desired response. Small variation of factors with high influence will result in high impact on the response. Also, influence of factors can be determined with P value, if P is less than 0.05 then factor has significance and if P value is greater, then factor is not significant [7, 8, 12]. If there is more than one response then multi response optimization is needed, one of methods used for this kind of optimization is Grey relation analysis. GRA converts multiple responses into a single response. At the end of GRA Grey relation grade is obtained, and combination of factors that has a highest value of grey relational grade is the closest to the optimal parameter setting.

First step of GRA is normalization of experiment results in range of 0-1. Depending if the minimization, maximization or nominal value of responses is needed there are three types of equations for normalization. In this study minimization of responses is needed so the normalization equation smaller-the-better is used, with following form:

$$x_i^*(k) = \frac{\max x_i(k) - x_i(k)}{\max x_i(k) - \min x_i(k)} \tag{1}$$

where $\max x_i(k)$ is maximum value of experiment response, $\min x_i(k)$ is minimum value of experiment response, $x_i(k)$ is original reference sequence, $i$ is number of experiments (in this case $i = 1...16$) and $k$ is number of responses ($k = 1$ for CoF, $k = 2$ for wear loss).

After normalization next step of GRA is calculation of Deviation sequence (equation 2) and finding Grey relational coefficients (GRC) for every experiment response with the use of equation 3.

$$\Delta_{0i}(k) = \left\| x_0^*(k) - x_i^*(k) \right\| \tag{2}$$

$\Delta_{0i}(k)$ is deviation sequence for reference sequence $x_0^*(k)$ and comparability sequence $x_i^*(k)$.

$$\xi_i(k) = \frac{\Delta_{\min} + \varphi\Delta_{\max}}{\Delta_{0i}(k) + \varphi\Delta_{\max}} \tag{3}$$

Where, as already said, $\Delta_{0i}(k)$ is deviation sequence for reference sequence $x_0^*(k)$ and comparability sequence $x_i^*(k)$, $\varphi$ is distinguishing coefficient ($0 < \varphi < 1$) and is taken as 0.5, $\Delta_{\min}$ and $\Delta_{\max}$ are the smallest value and the largest value of $\Delta_{0i}(k)$ respectively. After obtaining GRC for every experiment response Grey relational grade (GRG) can be calculated as:

$$\gamma_i = \frac{1}{n}\sum_{k=1}^{n} w_k \xi_i(k) \tag{4}$$

where $\gamma_i$ is the overall grey relational grade, $n$ is the number of test $w_k$, represents the weight factor for the *i*-th performance characteristic [13]. Weight factors are different for each parameter, because in real engineering importance of various factors is different, so obtaining them is very important in GRA. Most of researchers take that the weight factors are equal, but in this research will be taken in account real weight factor of parameters.

## 2. ANALYSIS AND DISCUSSION OF THE EXPERIMENTAL RESULTS

Based on the design of experiments tribological testing was conducted and experimental results for CoF and wear loss were obtained. It is important to mention that the parameters of experiment time and speed were constant and selected as 30 min and 100 rpm respectively. In this section results of Taguchi Grey analysis of obtained experimental results are presented. Within Taguchi analysis calculation of S/N ratios of the experimental results was done and is given in Table 2. S/N ratio for all experimental responses for CoF and wear loss is calculated and given in Table 2, while Table 3 and 4 show effect of each parameter on responses and order of their importance (Rank).

***Table 3*** *Response table for S/N ratios of CoF*

| Level | Parametres | | |
|---|---|---|---|
| | A | B | C |
| 1 | **10.699** | 10.813 | 9.102 |
| 2 | 10.569 | **11.717** | 9.597 |

| | | | |
|---|---|---|---|
| 3 | 10.281 | 9.144 | 11.210 |
| 4 | 10.387 | 10.261 | **12.026** |
| Delta | 0.419 | 2.573 | 2.924 |
| Rank | 3 | 2 | 1 |
| ∑delta | 5.916 | | |
| Weight | 0.24 | | |

Optimal combination of parameters for CoF is A1B2C4 i.e. 10N, 2 vol.% Gr and 4 vol.% $Al_2O_3$.

***Table 4*** *Response table for S/N ratios of wear loss*

| | Parametres | | |
|---|---|---|---|
| Level | A | B | C |
| 1 | **-18.69** | **-17.76** | -25.11 |
| 2 | -20.40 | -20.68 | -22.56 |
| 3 | -23.58 | -23.09 | -19.88 |
| 4 | -22.74 | -23.88 | **-17.86** |
| Delta | 4.89 | 6.11 | 7.25 |
| Rank | 3 | 2 | 1 |
| ∑delta | 18.25 | | |
| Weight | 0.76 | | |

Based on Table 4 minimal wear loss is achieved with A1B1C4 i.e. 10N, 1 vol.% Gr and 4 vol.% $Al_2O_3$ which is the optimal combination of parameters for wear loss.

### *2.1 Analysis of variance (ANOVA) and Grey relation analysis*

GRA was applied for investigation of wear behaviour of ZA27 nanocomposites. First normalization of responses was done, then deviation sequence and GRC were calculated with the use of equations 1-3. Normalized results and GRC are given in Table 5.

Next step, based on S/N analysis (Tables 3 and 4) and equation 5, weights of each response were obtained (24% and 76% for CoF and wear loss) and GRG was calculated with equation 6.

$$w_i = \frac{\sum_{j=1}^{p} Delta_{i,j}}{\sum_{i=1}^{m}\sum_{j=1}^{p} Delta_{i,j}} \quad (5)$$

where *m* is the number of response, *p* is the number of parameters and Delta presents the S/N ratio range from Table 3 and 4.

$$GRG = 0.24GRC_{CoF} + 0.76GRC_{WEAR\ LOSS} \quad (6)$$

GRG were calculated to determine the effects of parameters on the experiment results and ranked for each series (Table 5).

***Table 5*** *Results of Grey relational analysis*

| No. exp. | S/N ratio for CoF | S/N ratio for wear loss | NORM. CoF | NORM. Wear loss | Grey coefficient CoF | Grey coefficient Wear loss | GRG | RANK |
|---|---|---|---|---|---|---|---|---|
| 1 | 9.2877 | -19.8245 | 0.2925 | 0.8500 | 0.4141 | 0.7692 | 0.6840 | 9 |
| 2 | 11.4618 | -19.0849 | 0.7896 | 0.8833 | 0.7038 | 0.8108 | 0.7851 | 7 |
| 3 | 9.4867 | -20.0000 | 0.3434 | 0.8417 | 0.4323 | 0.7595 | 0.6810 | 10 |
| 4 | 12.5607 | -15.8478 | 0.9973 | 1.0000 | 0.9946 | 1.0000 | 0.9987 | 1 |
| 5 | 9.7596 | -16.2583 | 0.4112 | 0.9875 | 0.4592 | 0.9756 | 0.8517 | 3 |
| 6 | 10.6164 | -24.4022 | 0.6110 | 0.5667 | 0.5624 | 0.5357 | 0.5421 | 12 |
| 7 | 10.4580 | -19.2758 | 0.5755 | 0.8750 | 0.5408 | 0.8000 | 0.7378 | 8 |
| 8 | 11.4417 | -21.6557 | 0.7856 | 0.7542 | 0.6999 | 0.6704 | 0.6775 | 11 |
| 9 | 11.6306 | -18.9878 | 0.8233 | 0.8875 | 0.7388 | 0.8163 | 0.7977 | 5 |
| 10 | 12.5090 | -20.3407 | 0.9881 | 0.8250 | 0.9768 | 0.7407 | 0.7974 | 6 |
| 11 | 8.2237 | -26.6083 | 0.0000 | 0.3667 | 0.3333 | 0.4412 | 0.4153 | 14 |
| 12 | 8.7592 | - | 0.1517 | 0.1625 | 0.3708 | 0.3738 | 0.3731 | 15 |

| | | | | | | | | |
|---|---|---|---|---|---|---|---|---|
| | | 28.3991 | | | | | | |
| 13 | 12.5759 | -15.9868 | 1.0000 | 0.9958 | 1.0000 | 0.9917 | 0.9937 | 2 |
| 14 | 12.2824 | -18.8897 | 0.9472 | 0.8917 | 0.9044 | 0.8219 | 0.8417 | 4 |
| 15 | 8.4076 | -26.4856 | 0.0531 | 0.3792 | 0.3456 | 0.4461 | 0.4220 | 13 |
| o. exp. | S/N ratio for CoF | S/N ratio for wear loss | ORM. CoF | ORM. Wear loss | Grey coefficient CoF | Grey coefficient Wear loss | RG | ANK |
| 6 | .2815 | 29.6001 | .0168 | .0000 | 0.3371 | 0.3333 | .3342 | 6 |

The variation of grey relation grade results is shown in Figure 1. Maximum tribological characteristics for all experimental investigations can be found for case when grey relation grade is the highest. In this investigation, it is seen that for experiments number 4 and 13 are obtained maximum tribological characteristics. The best optimal characteristic was found based on the ranking in Table 5.

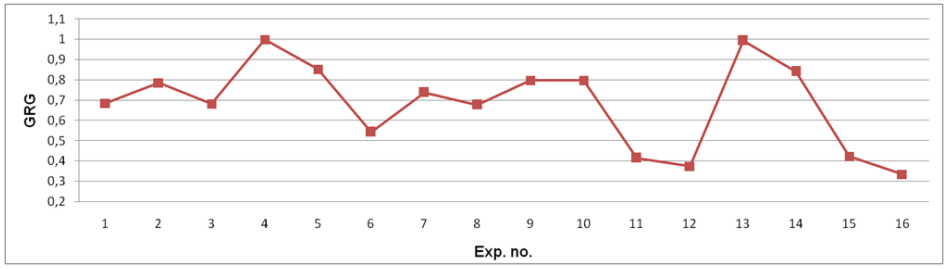


*Figure 1 Grey relation grade for the maximum tribological characteristics*

The GRC, GRG and the rank of each experiment were found from Eqs. (1) – (6), and the results are shown in Table 5. These results are in accordance with Table 6, which is the response table for the grey relational grade. The optimum level of each experiment parameter is bolded value given in Table 6 and shown in Figure 2.

***Table 6*** *Response table for grey relational grade*

| Level | Parameters | | |
|---|---|---|---|
| | A | B | C |
| 1 | **-2.187** | **-1.678** | -6.442 |
| 2 | -3.184 | -2.721 | -4.888 |

| | | | |
|---|---|---|---|
| 3 | -5.031 | -5.276 | -2.545 |
| 4 | -4.641 | -5.369 | **-1.168** |
| Delta (max-min) | 2.844 | 3.691 | 5.274 |
| Rank | 3 | 2 | 1 |

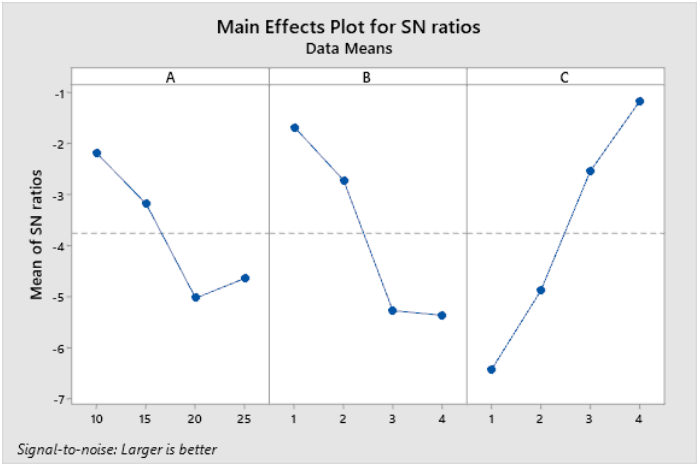


*Figure 2 Effect of each parameter on multiple responses*

According to the GRG given in Table 5 optimum value was obtained at A1B4C4, with the rank 1. However from Table 6 main optimum levels of the parameters were obtained at A1B1C4 according to the mean GRG. This happens because design of experiment by which there are not needed all combinations of parameters, but with great reliability optimum parameter levels can be achieved with little experimental data by using Taguchi based GRA which will be proven with confirmation test. To investigate the significance of load, reinforcement Gr and reinforcement $Al_2O_3$ on the tribological characteristics, the analysis of variance (ANOVA) was conducted for the average GRG responses at the 95% confidence level. The results of GRG are evaluated within the ANOVA method and contribution ratios of each parameter are presented in Table 7. Statistical effect of all observed parameters was obtained. Last column of Table 7 shows the contribution percentage (%) of each parameter on the GRG. ANOVA analysis shows that the highest effect has reinforcement content $Al_2O_3$, and then effect of reinforcement content Gr on multi response optimization of tribological characteristics with 48.61% and 30.07 %, respectively. The least effect with 15.17% has load, while error has effect of 6.16%. On the Figure 3 are ilustrated the response contour plots for illustrating effects of load, reinforcement content Gr and $Al_2O_3$ on GRG.

***Table 7*** *Analysis of Variance for Grey relational grade*

| Parameters | DOF | Seq SS | Adj SS | AdjMS | F | P | Contribution (%) |
|---|---|---|---|---|---|---|---|
| A | 3 | 20.793 | 20.793 | 6.931 | 4.93 | 0.047 | 15.17 |
| B | 3 | 41.217 | 41.217 | 13.739 | 9.77 | 0.010 | 30.07 |

| | | | | | | | |
|---|---|---|---|---|---|---|---|
| C | 3 | 66.640 | 66.640 | 22.213 | 15.79 | 0.003 | 48.61 |
| ResidualError | 6 | 8.441 | 8.441 | 1.407 | | | 6.16 |
| Total | 15 | 137.091 | | | | | 100.00 |

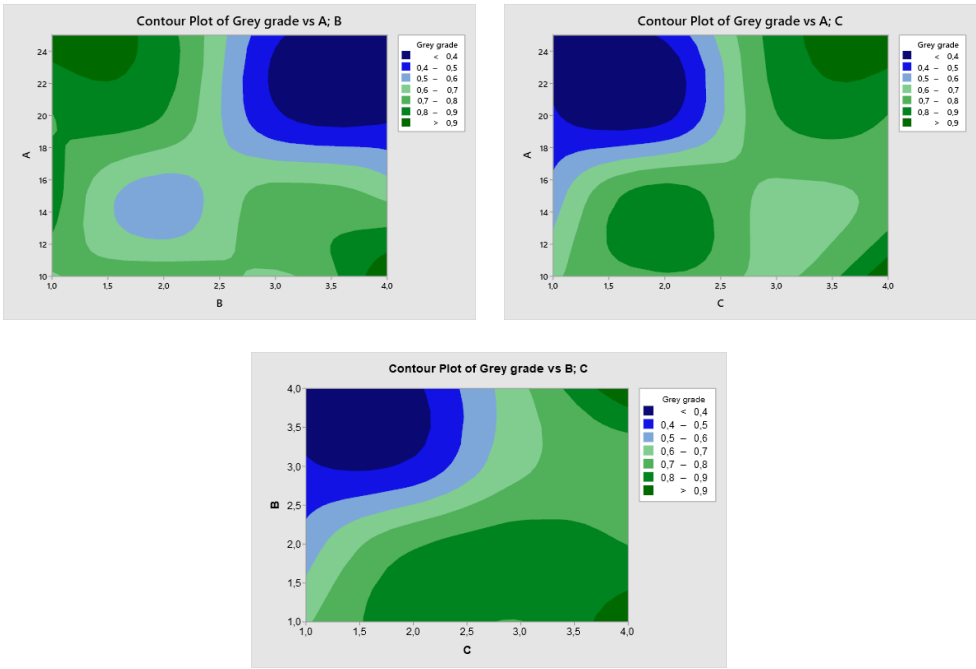


*Figure 3 Effect of each parameter interactions on GRG: a) Effect of load and content of Gr, b) Effect of load and content of Al2O3, c) Effect of content of Gr and content of Al2O3*

The effect of parameters on GRG can be determined based on shades of two colors (blue and green) i.e. deep green shows the highest effect of parameter interaction on GRG while deep blue shows the least effect of parameter interaction on GRG. Interection between load and content of Gr (Figure 3a) shows that GRG is the highest for load of 10 N and content of 4 vol.% Gr. The same applies for interaction between load and content of $Al_2O_3$ (Figure 3b) the highest GRG is for load of 10 N and content of 4 vol.% $Al_2O_3$. As for effect of the interaction between reinforcement contents of Gr and $Al_2O_3$ (Figure 4) highest GRG is for 1 and 4 vol.% Gr and 4 vol.% $Al_2O_3$, which is according to optimal combinations obtained with Taguchi Grey analysis.

### *2.2 Confirmation experiments*

The last and very important step of multi response optimization is confirmation experiment for optimal parameters level. The purpose of confirmation test is to validate conclusions from analysis stage. In Taguchi Grey analysis confirmation test is done if optimal combinations of parameters are different between GRA and S/N. Optimal parameter combination with GRG and S/N was A1B4C4 and A1B1C4 respectively. Because combination A1B1C4 was not done experimentally in orthogonal array, confirmation

experiment was done for this combination. Results of confirmation test for optimum parameters are given in Table 8.

***Table 8*** *Analysis of Variance for Grey relational grade*

| Optimal combination | Experiment | | Prediction | |
|---|---|---|---|---|
| A1B1C4 | Experimental results | GRG for experimental value | Results | GRG |
| CoF | 0.21592 | 1 | 0.216 | 0.9986 |
| Wear loss | 4.6 | | 4.61 | |

After the experiment CoF and wear loss were 0.21592 and 4.6 respectively. Then GRG was calculated as 1 which proves that this is the optimal combination of parameters. Prediction of GRG with the use of Taguchi was done as well and value of GRG was 0.9986 which is very close to the GRG of experimental value. Based on prediction of GRG values for CoF and wear loss were calculated and they are very close to experimental ones and they are presented in Table 8.

## 3. CONCLUSIONS

Based on the results in this study it can be concluded that Taguchi based Grey relational analysis is very useful tool for multi response optimization of tribological behaviour of zinc based nanocomposites with different reinforcement content. Observed responses of this investigation were CoF and wear loss. Because there was more than one response, in order to optimize these nanocomposites, the multi response methods are applied. In this paper GRA is used for multi response optimization of parameters load, content reinforcements $Al_2O_3$ and Gr on tribological behaviour nanocomposite. The highest GRG was obtained for combination A1B4C4 more precisely 10N, 4 vol.% Gr and 4 vol.% $Al_2O_3$. From analysis of S/N ratio of GRG different combination was obtained noted as A1B1C4 i.e. 10N, 1 vol.% Gr and 4 vol.% $Al_2O_3$. Confirmation experiment validated the improvement of CoF and wear loss for combination obtained by S/N. From the ANOVA analysis of GRG it is noted that reinforcement content of $Al_2O_3$ is the most significant parameter affecting the tribological behaviour of nanocomposites with 48.61%, following reinforcement content of Gr and load with 30.07% and 15.17%, respectively. Future research can be focused on investigation of influence of the wider range of reinforcement content on the composites' properties. It is also possible to do multi optimization by observing tribological and mechanical properties in order to obtain materials with the best characteristics.

## ACKNOWLEDGMENTS

The paper was written during research funded by the Ministry of Education, Science and Technological Development. Besides, the authors of the present study thank to TÜBİTAK (Scientific and Technological Research Council of Turkey) for their financial support of the projects with the Project Number 213M276.

## REFERENCES

[1] Veličković, S., Stojanović, B., Ivanović, L., Miladinović, S., Milojević, S.: "Application of nanocomposites in the automotive industry", Mobility and Vehicle Mechanics, 2019, Vol. 45, No. 3, pp. 51-64. Doi: 10.24874/mvm.2019.45.03.05.

[2] Vučetić, F., Veličković, S., Milivojević, A., Vencl, A.: "A review on tribological properties of microcomposites with ZA-27 alloy matrix", 15th International Conference on Tribology – Serbiatrib'17, Faculty of Engineering University of Kragujevac, Kragujevac, Serbia, 2017, 17 – 19 May, pp. 169-176.

[3] Babic, M., Stojanovic, B., Dzunic, D., Pantic, M.: "Micro/nanoscale structural, mechanical and tribological characterization of ZA-27/SiC nanocomposites", Journal of Composite Materials, 2020, Vol. 54, No. 16, pp. 2113-2129. Doi: 10.1177/0021998319891766.

[4] Güler, O., Cuvalci, H., Canakci, A., Celebi, M.: "The effect of nano graphite particle content on the wear behaviour of ZA27 based hybrid composites", Advanced Composites Letters, 2017, Vol. 26, No. 2, pp. 30-36. Doi: 10.1177/096369351702600201.

[5] Pul, M.: "Effect of sintering temperature on pore ratio and mechanical properties of composite structure in nano graphene reinforced ZA27 based composites", International Journal of Minerals, Metallurgy and Materials, 2020, Vol. 27, pp. 1-12. Doi: 10.1007/s12613-019-1926-2.

[6] Kumar, N. S.: "Mechanical and wear behavior of ZA-27/Sic/Gr hybrid metal matrix composites", Materials Today: Proceedings, 2018, Vol. 5, No. 9, pp. 19969-19975. Doi: 10.1016/j.matpr.2018.06.363.

[7] Almomani, M. A., Hayajneh, M. T., Alelaumi, S. M.: "Applying Taguchi method to study the wear behaviour of ZA-27 alloy-based composites reinforced with SiC nanoparticles", International Journal of Cast Metals Research, 2019, Vol. 32, No. 4, pp. 229-241. Doi: 10.1080/13640461.2019.1643061.

[8] Shivakumar, N., Vasu, V., Narasaiah, N.: "Processing and dry sliding wear behavior of Al2O3 nanoparticles reinforced ZA-27 composites", Materials Today: Proceedings, 2017, Vol. 4 No. 2, pp. 4006-4012. Doi: 10.1016/j.matpr.2017.02.302.

[9] Bobić, B., Vencl, A., Ružić, J., Bobić, I., Damnjanović, Z.: "Microstructural and basic mechanical characteristics of ZA27 alloy-based nanocomposites synthesized by mechanical milling and compocasting", Journal of Composite Materials, 2019, Vol. 53, No. 15, pp. 2033-2046. Doi: 10.1177/0021998318817876.

[10] Karimzadeh, F., Enayati, M. H., Tavoosi, M.: "Synthesis and characterization of Zn/Al2O3 nanocomposite by mechanical alloying", Materials Science and Engineering: 2008, A, Vol. 486, No. 1-2, pp. 45-48. Doi: 10.1016/j.msea.2007.08.059.

[11] Güler, O., Çuvalcı, H., Gökdağ, M., Çanakçi, A., Çelebi, M.: "Tribological behavior of ZA27/Al2O3/graphite hybrid nanocomposites", Particulate Science and Technology, 2018, Vol. 36, No. 7, pp. 899-907. Doi: 10.1080/02726351.2017.1326994.

[12] Veličković, S., Stojanović, B., Babić, M., Bobić, I.: "Optimization of tribological properties of aluminum hybrid composites using Taguchi design", Journal of composite materials, 2017, Vol. 51, No. 17, pp. 2505-251. Doi: 10.1177/0021998316672294.

[13] Dey, A., Debnath, S., Pandey, K. M.: "Optimization of electrical discharge machining process parameters for Al6061/cenosphere composite using grey-based hybrid approach", Transactions of Nonferrous Metals Society of China, 2017, Vol. 27, No. 5, pp. 998-1010. Doi: 10.1016/S1003-6326(17)60117-1.

**MOBILITY & VEHICLE MECHANICS**

DOI: 10.24874/mvm.2021.47.03.03
**UDC: 622.7.092:621.43**

# STATIONARY TEST PLAN OPTIMISATION USING SLOW DYNAMIC SLOPE ENGINE SCREENING

*Predrag Mrđa[1]*, Nenad Miljić[2], Slobodan Popović[3], Marko Kitanović[4]*

*Received in July 2020* *Revised in September 2020* *Accepted in February 2021*

RESEARCH ARTICLE

**ABSTRACT:** Requirements regarding high fuel efficiency, low pollutants and $CO_2$ emission impact of the internal combustion (IC) engine results in high control calibration complexity. Modern IC engines are equipped with numerous electronically controlled subsystems, whose usage leads to almost exponential growth of stationary operating points that need to be evaluated and optimised. In that perspective, the methodology for fast pre-knowledge acquisition of examined system is presented through the application of Slow Dynamic Slope experiments – SDS. Continual slow change of a control parameter excites the system, in such a way, that allow obtaining of an approximately stationary operating regime, without the time-consuming operating point settling period. By analysing stationary-based approximation results of Slow Dynamic Slope experiments, conducted within the IC engine global operation domain (engine speed and load), certain zones could be identified. Within those zones, increased number of stationary tests is desirable in order to provide a more precise approximative model of observed engine output parameters. In this way, relatively fast dynamic SDS experiments could be used to optimise the stationary-based test plan leading to overall time savings dedicated to IC engine testing.

**KEY WORDS**: internal combustion engine, dynamic engine testing, slow dynamic slope, stationary based approximation, stationary test plan



[1]*Predrag Mrđa, M.Sc., Research assistant, University of Belgrade, Department of Internal Combustion Engines, Faculty of Mechanical Engineering, Kraljice Marije 16, 11120 Belgrade 35, Serbia, pmrdja@mas.bg.ac.rs (*Corresponding author)*
[2]*Nenad Miljić, PhD., assoc. prof., University of Belgrade, Department of Internal Combustion Engines, Faculty of Mechanical Engineering, Kraljice Marije 16, 11120 Belgrade 35, Serbia, nmiljic@mas.bg.ac.rs*
[3]*Slobodan Popović, PhD., assoc. prof., University of Belgrade, Department of Internal Combustion Engines, Faculty of Mechanical Engineering, Kraljice Marije 16, 11120 Belgrade 35, Serbia, spopovic@mas.bg.ac.rs*
[4]*Marko Kitanović, M.Sc., Research assistant, University of Belgrade, Department of Internal Combustion Engines, Faculty of Mechanical Engineering, Kraljice Marije 16, 11120 Belgrade 35, Serbia, mkitanovic@mas.bg.ac.rs*

# STACIONARNI TEST PLAN OPTIMIZACIJE PRAĆENJA KARAKTERISTIKE OPTEREĆENJA MOTORA SA MALIM KONSTANTNIM GRADIJENTOM PORASTA OPTEREĆENJA MOTORA

**REZIME**: Zahtevi u vezi sa visokom efikasnošću goriva, niskim zagađivačima i uticajem emisije $CO_2$ na motor sa unutrašnjim sagorevanjem (IC) rezultiraju velikom složenošću kontrole kalibracije. Savremeni IC motori opremljeni su brojnim elektronski kontrolisanim podsistemima, čija upotreba dovodi do gotovo eksponencijalnog rasta stacionarnih radnih tačaka koje je potrebno proceniti i optimizovati. U toj perspektivi, metodologija za brzo sticanje predznanja ispitivanog sistema predstavljena je primenom eksperimenata sa malim konstantnim gradijentom porata opterećenja (SDS). Kontinualna spora promena upravljajućeg parametra pobuđuje sistem tako da se dobija približno stacionaran režim rada, bez dugotrajnog perioda formiranja radne tačke. Analizom rezultata približno stacionarnog eksperimenata sa malim konstantnim gradijentom, sprovedenih u uobičajenom radnom režimu rada motora IC (broj obrtaja motora i opterećenje), mogle bi se identifikovati određene zone. Unutar tih zona, poželjan je povećan broj stacionarnih ispitivanja kako bi se obezbedio precizniji približni model posmatranih parametara izlazne snage motora. Na ovaj način, relativno brzi dinamički SDS eksperimenti mogli bi se koristiti za optimizaciju plana stacionarnog ispitivanja što dovodi do ukupne uštede vremena neophodnog za testiranje IC motora.

**KLJUČNE REČI**: motor sa unutrašnjim sagorevanjem, dinamičko ispitivanje motora, mali konstantni gradijent porasta opterećenja, stacionarna aproksimacija, plan stacionarnog ispitivanja

# STATIONARY TEST PLAN OPTIMISATION USING SLOW DYNAMIC SLOPE ENGINE SCREENING

*Predrag Mrđa, Nenad Miljić, Slobodan Popović, Marko Kitanović*

## INTRODUCTION

Dynamic testing of internal combustion (IC) engines has been applied in the world for decades in the process of control parameters calibration. Taking into consideration the share of battery electric vehicles (BEV) on the market and predictions related to propulsion systems of the future, IC engines will maintain the dominant portion [1, 2] as the primary propulsion technology of civil and commercial transportation. Given that IC engines are, in most cases, used in dynamic operation conditions, research in this area is of great importance. The basic idea of the Slow Dynamic Slope (SDS) method is to obtain approximate values of stationary approximations of the observed measured values in a much faster way, compared to stationary engine testing. The differences of the stationary approximations obtained in this way, compared with the results of the stationary test is expected because the IC engine could be represented as an extremely nonlinear dynamic system, with elements of stochastic processes. Because of this reason, unlike dynamic, stationary tests are the most reliable source of information about the work cycle at each operating point of an IC engine or a propulsion system generally. Considering increasingly demanding limitations that are required for modern IC engines, especially in terms of fuel economy and exhaust gases composition, further complexity increase of the propulsion systems is certain. Complex drive systems are characterized by an extremely high number of control parameters combinations. Testing of all those combinations on the test bench in stationary conditions cannot be realized within a reasonable time, and the economic framework. In this sense, the proposed analysis of the results of the SDS method has a favourable effect on the reduction of the number of operating regimes at which it is necessary to test the IC engine, while maintaining the quality of the approximation.

## 1. SLOW DYNAMIC SLOPE METHODS

Numerous papers on the topic of IC engine testing and modelling as a complex nonlinear and dynamic system, confirm the real need of the industry for further research in this area [3, 4, 5]. Dynamic tests of IC engines, based on the method of the continual control parameter change by ramp function are relatively old [6], but with the development of IC engine test bench systems, the potential of those methods increases. In the paper [7] the results of the IC engine dynamic testing using the SDS method over the engine load parameter are presented. The load is varied continuously in the area of positive torque with short-term retention at the minimum and maximum absolute values of the control parameter. Also, paper [7] presents the results of two, relatively fast SDS cycles, with symmetrical slopes of the control parameter focusing on the response trace of the exhaust gas NOx content. In addition to monitoring the response of IC engine effective parameters in the global domain (speed and load), in [8] the SDS method was applied for the purpose of optimizing the ignition angle and distribution system parameters of an IC engine. In other words, quantities that are a function of global control variables are used as a sweep parameter. For such a research to be conducted, the test bench at AVL Research Centre was equipped with engine control unit (ECU) capable of performing controlled sweeps of engine control parameters. Particularly positive results in the field of application of SDS methodology were elaborated in the paper [9], which was created through the cooperation of

the automotive industry - BMW and AVL. In that paper, special attention is given to the calibration of control parameters near the safe operation boundary, i.e. safe region for the tested engine and used measuring equipment. MAZDA, as one of the leading companies in terms of innovation in the global automotive industry, has also, in cooperation with AVL, conducted research in this field [10]. The optimization of diesel engine control in transient modes was analysed using a similar method and presented in the dissertation [11]. As part of this research, the author devoted himself to the analysis of very fast changes in fuel injection quantities, defined by slope functions in the time domain over the successive work cycles in order to study the system response in terms of effective torque and possible corrections and maintaining the desired mixture composition. HONDA engineers, through research [12], published the results of stationary approximation of particulate emissions of gasoline engine with direct injection using SDS methodology introducing dynamic control of the start of injection (SOI) parameter in the crank angle domain. Also, in that research, an SDS method with variable gradients within a single dynamic sweep was applied, in order to apply a smoother change within areas where higher particulate emissions are expected. The potential of SDS methodology has not been fully explored and further research is still being done to improve it. The latest researches are those conducted through the cooperation of the Department of Engines at the Faculty of Mechanical Engineering in Belgrade and AVL from 2015 [13].

By analysing the available literature and published research results, the advantages and disadvantages, as well as the assumptions that could be applied during engine testing, are clearly distinguished. The general idea of applying a dynamic test of an IC engine, with a relatively slow change of the control parameter, is that the results of such a test completely replace the results of the stationary examination in the domain of varied control parameter. Unfortunately, some IC engine operating processes have a distinct time constant, i.e. they react relatively slowly to the changes of the input parameter. Those values could be tested and evaluated in SDS way, but only with limited accuracy levels due to significant deviation from stationary test results. On the other hand, it can be shown that with the SDS method and with the usage of adequate measuring techniques, it is possible to form very precise stationary approximations. Additionally, if the observed engine parameter is characterized by a relatively fast dynamic response, the match with stationary experimentation is acceptable.

Within the framework of this paper, the main goal of applied SDS method, is implementation of preliminary steps for more effective definition of the stationary test plan. In doing so, the level of prior knowledge about the examined IC engine, or any other system under test, will increase rapidly utilising this type of dynamic test. In the publication [3] and in the previous research of the authors [14, 15], the theoretical foundations of the SDS mode of excitation are presented. Figure 1 shows the SDS excitation $u(t)$ and the response $y(t)$ of an arbitrary linear system. Also, the stationary characteristic of such a system, the dynamic response as a function of excitation and the middle line of the formed SDS trace are shown. The stationary characteristic can be interpreted as the response of a system with negligibly small time constant $(T_1 = 0)$.

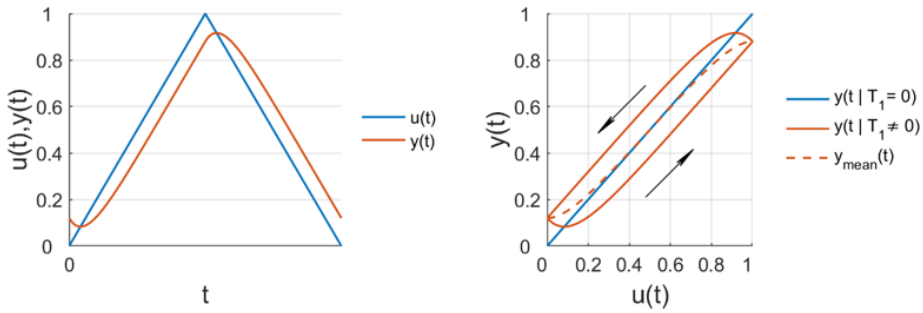


*Figure 1 Example of excitation and the arbitrary first order linear system response by means of SDS test*

It is noticed that in a relatively wide range of the input values, matching of stationary response and the midline of the SDS envelope is relatively good. In practice, the results are different and strongly depend on system dynamics and nonlinearity, but the analogy with the response analysis of a first-order linear system is evident. In that manner, an identical conclusion can be drawn when considering an example of a nonlinear system with first order dynamics. The example of nonlinear system is formed using simple Hammerstein-Wiener model and comparative analysis is shown in the Figure 2. SDS excitation and the system response are given in the time domain, alongside overlapped system stationary characteristics and the middle line of SDS trace.

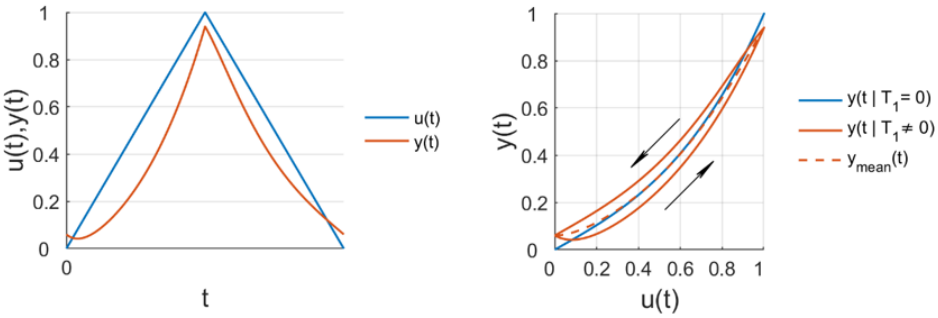


*Figure 2 Example of excitation and the arbitrary first order nonlinear system response by means of SDS test*

By analysing the deviations of the actual stationary characteristics and approximations obtained through the SDS experiment, the potential and benefits of the SDS method, as a way of IC engine testing method, could be identified. Relatively fast dynamic tests with a slow change of the control parameter can provide the collection of a large amount of information about the tested object in a very short time. How small the difference between the SDS results will be, comparing to the actual stationary values, depends on many factors, such as the dynamics of the observed process and the slope of the SDS excitation ramp. Of course, the excitation slope factor affects the duration of the dynamic experiment (i.e. the cost of the experiment), but this parameter is certainly a matter of compromise.

In previous research by the authors [14, 15], a comparative analysis of the different slopes (and thus durations) of SDS ramps were given and the different ways of preparing the IC engine before the main part of the dynamic sweep were analysed. In these researches, the focus was on stationary and dynamic system preparation in terms of engine load variations during SDS experiment and for engine speed kept at constant level.

## 2. ENGINE TEST BENCH SETUP

Systems used for in-laboratory IC engine testing are very complex. The process of testing modern IC engines would be practically impossible without a certain level of system automation. Automated monitoring and display of measured values provides insight into the operating parameters of the used laboratory installation, with the possibility of checking limit values, such as the maximum allowable exhaust temperature or the allowable level of detonation in the cylinder, during adjusting phase of the operating point. In addition to the protection of the engine and measuring equipment, by monitoring other measured values, it is possible to detect malfunctions on the installation, in a timely manner, thus avoiding the need to repeat the measurement. Automated data collection into files has long been standard in engine testing. In this way, it is possible to calculate the statistical parameters of the measured quantities over an arbitrary population of data in terms of mean value, standard deviation, coefficient of variation and the like. If the test plan is extensive, which implies long-term testing, systems for automated experimentation without permanent operator supervision are applied. Automated IC engine testing plans are implemented using commercially available software AVL CAMEO [16]. The basic functionality of AVL PUMA Open software, in terms of communication between the AVL CAMEO software and the dyno controller, was implemented within the NI LabVIEW programming environment. AVL CAMEO software is an engineering tool that enables complete control of the test bench for engine testing, calibration of control parameters and formation of simple mathematical models of parameters that characterize the IC engine working process. Figure 3 shows the schematics of software and application units for automated adjustment of the operating point of the IC engine realized at the Department of Engines of the Faculty of Mechanical Engineering in Belgrade.

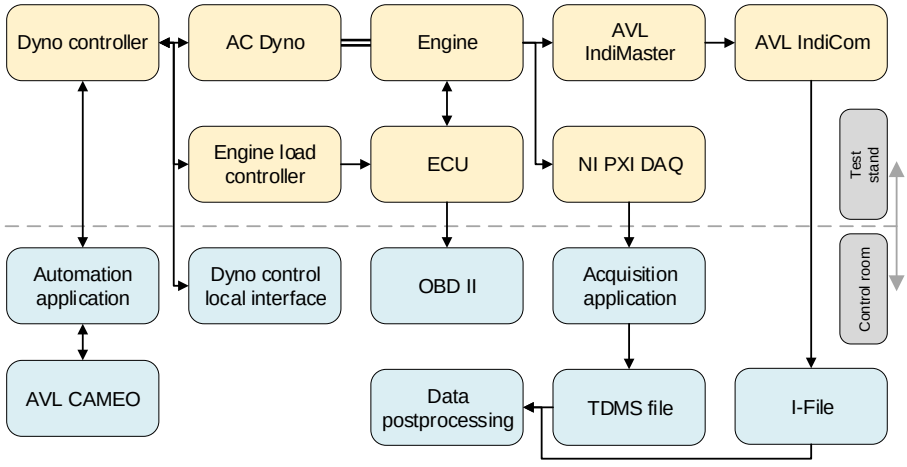


*Figure 3 Engine test bench systems configuration*

The engine is connected to the dynamometer via a shaft mounted torque-meter. The brake controller parameters, as well as the ECU parameters, are accessed via a test automation application. Time domain data acquisition is based on the NI PXI hardware and LabView software. The AVL IndiMaster platform, AVL 3064Z01 encoder, AVL Micro IFEM 4P4G charge amplifiers with the corresponding AVL IndiCom software is used to indicate in-cylinder pressure values. Post-processing of time domain acquisition data (TDMS files) and engine indication data (IFiles) gives the final datasets for stationary and dynamic tests. The IC engine and the dynamometer basic features are shown in the Table 1.

***Table 1*** *IC engine and dyno basic features*

| | | |
|---|---|---|
| IC Engine | manufacturer | PSA group |
| | type | DV4TD |
| | fuel type | diesel |
| | injection type | direct injection (HDI) |
| | displacement | 1398 cm3 |
| | piston bore / stroke | 73.7 mm / 82.0 mm |
| | compression ratio | 18:1 |
| | max. performance | 40 kW@4000 min-1, 130 Nm@1750 min-1 |
| | turbocharger | BorgWarner KP35 (3K-BW), no intercooler |

| | | |
|---|---|---|
| Dyno | manufacturer | Rotronics |
| | type | Dynosens |
| | AC motor | SCHORCH LN8280M-A |
| | max. performance | 300 kW@9200 min-1, 720 Nm@540-4200 min-1 |
| | max. rotational speed | 10000 min-1 |

## 3. SDS TEST RESULTS INTERPRETATION

As an example of the SDS test results analysis, the engine intake manifold pressure trace, at the section after of the compressor, was taken. In the following, this channel is marked as P_21. Figure 4 shows the envelope of the pressure trace during the SDS experiment at 1500 [$min^{-1}$] for different inclinations of the engine load, i.e. different durations of the SDS experiment for the desired load range (from 0 [Nm] to the maximal load of 115 [Nm]). The

results shown in this figure correspond to the setting of a dynamic test as a repeatable input parameter (load) oscillation. Also, a line corresponding to the P_21 stationary characteristic in these regimes is given. On the right-hand side of the Figure 4 the relative difference of the SDS test envelope middle line in comparison to the stationary values of the P_21 parameter is shown.The physicality of the working process and the characteristics of the measuring equipment in terms of its ability to react quickly enough on the control parameter changes lead to approximately equal values of the relative difference of the middle line of the SDS envelope in comparison to the stationary test. For the observed parameter, the largest output differences, in terms of SDS test duration, are observed at higher loads for a given engine speed. Numerical values in line label correspond to SDS duration, thus D120 means that effective part of SDS test lasted 120 seconds. Since it is a turbocharged engine, any delay of the temperature rise (and fall) in the exhaust system directly affects the rate of increase of the enthalpy of exhaust gases, and the amount of energy that will be transferred to the compressor unit depends on the energy of the exhaust gases, which further reflects on the values of the parameter P_21.

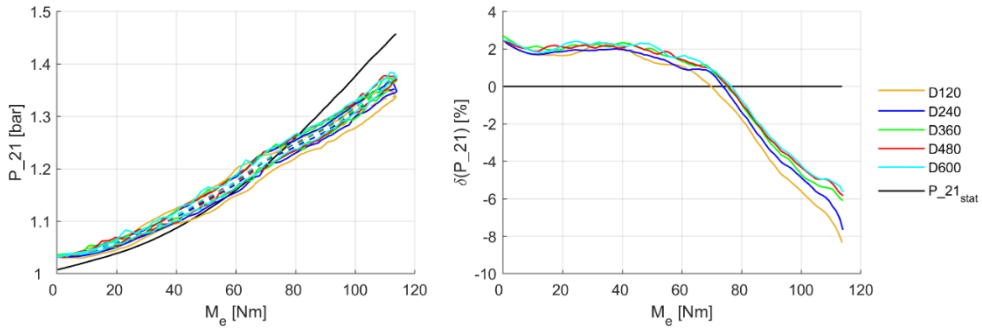


*Figure 4 Intake manifold pressure traces (P_21) for various SDS test durations and SDS middle line relative differences in relation to stationary values ($P\_21_{stat}$) at 1500 [$min^{-1}$]*

The intake manifold absolute pressure P_21 is selected as an example because this parameter possess relatively fast dynamic response and a sufficiently large magnitude of change as a function of the independent control variables (engine speed and load). Figure 5 shows a stationary approximation of this parameter for the shortest SDS test duration. In the same figure, on the right-hand side, the relative difference of P_21 in comparison with the stationary data is shown. It is noticed that the deviation for the most part is about ±2%. It should not be forgotten that the universal diagram was recorded with four SDS sweeps (at engine speeds 1500, 2000, 2500 and 3000 [min-1]) and that each of them lasted 2 minutes. The data needed for the universal characteristics diagram in Figure 5 were obtained in approximately 10 minutes of engine testing.

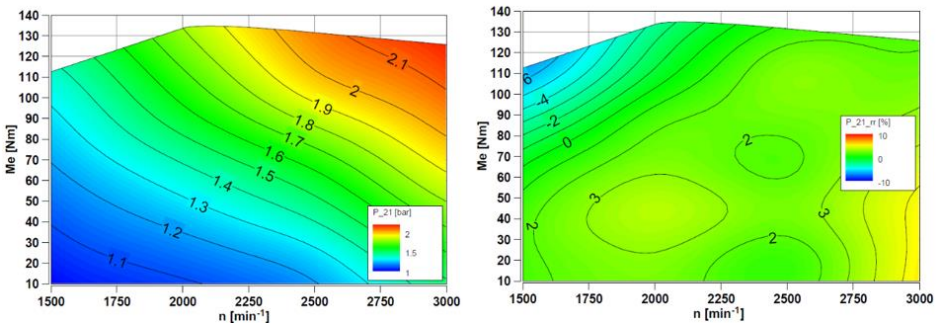


*Figure 5 Intake manifold pressure P_21 universal characteristics obtained by SDS method, and relative diferencess od this paramater compared to stationary exsamination (P_21_rr)*

## 4. KEY STATIONARY TEST POINTS BASED ON SDS RESULTS

If there is a nonlinear stationary characteristic that needs to be identified using experimental methods, the points of the stationary test-plan need to be distributed as uniformly as possible regarding the quality of used fitting model. It is also desirable that the test points be selected by one of the known quasi-random methods, such as Sobol or Halton sequences, so that the test-plan can be expanded if needed.

The correct selection of test-plan points is as important as the selection of appropriate mathematical model for approximations formation. For systems with distinct nonlinearity, it is desirable that a larger number of test points be positioned in the areas of higher absolute values of the second derivative of the observed nonlinearity [17], which for system with one input can be defined as:

$$\nabla^2 y(u) = \frac{\partial^2}{\partial u^2}\vec{e}_{u_1} \tag{1}$$

For systems with two independent inputs, the combined value of output first derivative could be defined as:

$$\nabla y(u_1, u_2) = \frac{\partial y}{\partial u_1}\vec{e}_{u_1} + \frac{\partial y}{\partial u_2}\vec{e}_{u_2} \tag{2}$$

by determining the Euclidean distance, an argument is obtained for determining the second derivative:

$$\nabla^2 y(u_1, u_2) = \nabla\|\nabla y(u_1, u_2)\| = \frac{\partial^2 y}{\partial u_1^2}\vec{e}_{u_1} + \frac{\partial^2 y}{\partial u_2^2}\vec{e}_{u_2} \tag{3}$$

By determining intensity of the observed function second derivative, finding the absolute value and normalization, the function that quantifies the areas for adding points on the whole domain of independent input variables u_1 and u_2 is obtained in form:

$$F(u_1, u_2) = \text{norm}\big(abs(\|\nabla^2 y(u_1, u_2)\|)\big) \tag{4}$$

Figure 6 shows the values of such a function (F(u_1,u_2 )), which quantifies the area for adding the test-plan points based on the analysis of the pressure values in the intake manifold (P_21) gathered during stationary engine examination. For simplification, this

function will be named "condition function" in the following lines. In addition, Figure 6 shows submodels (boundaries and central positions) of the global LOLIMOT approximation model [18]. In this case, a relatively complex LOLIMOT model with 80 submodels was formed, because it enables a more precise comparison of IC engine global subregions. It is noticed that there is a certain coincidence between the areas of more intensive condition function values and the areas in which the multiple partitioning of the LOLIMOT model. In these areas, the linear function of the LOLIMOT submodel, although weighted by the σ function, approximates the source data with a higher value of the mean square deviation. The consequence of this scenario is the partitioning of the LOLIMOT submodel, which enables a more flexible approximation, i.e. an approximation that will better accompany the observed data. Also, Figure 6 shows the iso-contour of the condition function that delimits the IC engine global operation space according to a predefined ratio of 30%:70%.

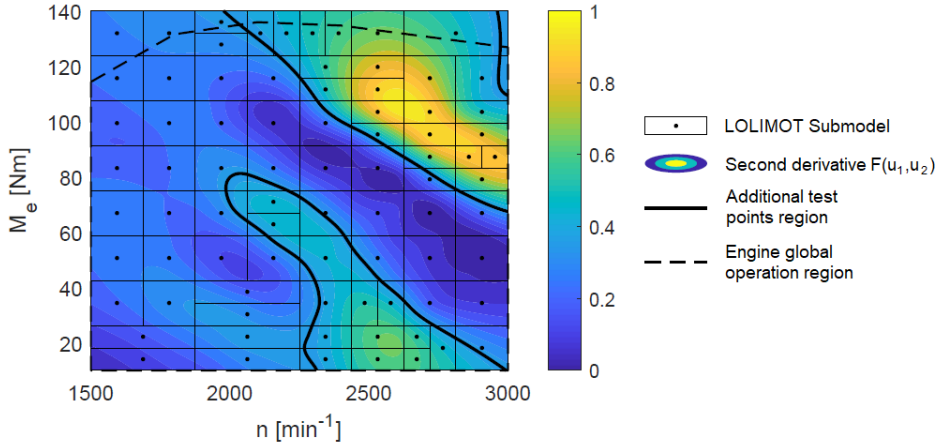


*Figure 6 Quantification of the area for adding test points, the position of the LOLIMOT approximation submodels and dividing boundary of higher and lower test points population based on P_21 parameter*

The shown share of the IC engine operating domain is empirically determined as a compromise between the minimum allowable distance between design points, the number of starting points and the points added to the test plan for a given dimension of the input domain. Equation 4 is given in the index notation and thus allows determination of condition function in n-dimensional space, which for higher dimensionality of the global operation space means defining hyper-space to add test-plan points. The processed nonlinearity, i.e. the required IC engine universal characteristic, is unknown at the moment of the design of experiment, and the usage of SDS testing methodology as a way of collecting knowledge about the system under test can contribute in that sense. The results of the SDS tests cannot replace the stationary obtained data, but they can approximate the shape of nonlinearity and indicate areas within which it would be desirable to increase the number stationary test plan points. In contrary, this method can also indicate regions of insignificant experiment configuration, which leads to test plan reduction and thus to experimentation efficiency improvement. By analysing data of intake manifold pressure, obtained using SDS test methods, the areas for adding significant points into stationary test plan, are shown in the Figure 7. The measuring chain used for P_21 pressure readings, is characterized by a relatively fast response, so positions of the calculated areas are similar to that obtained by the stationary testing results. It is noticed that the approximation determined on the basis of

the SDS test with the slowest control parameter rate of change (the longest test marked as D600) has a relatively good match with reference stationary results analysis. Test marked as D120, is characterized by the fastest execution, and slight mismatch with reference data is noticeable, but still, there is great coincidence to stationary data in general.

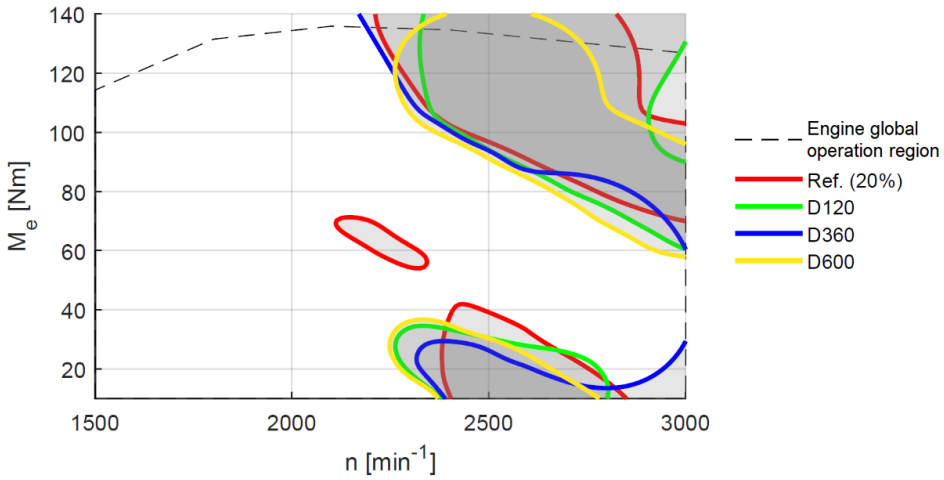


*Figure 7 Areas for adding most significant test points based on reference stationary tests results and based on SDS tests of different durations for the P_21 output parameter*

## 5. CONCLUSIONS

IC engine testing, using the SDS methodology, has the best results if the observed output parameter is characterized by a relatively short settling time, i.e. fast dynamic response. It is found that this category includes pressure and flow measurements in the time domain, as well as engine cylinder pressure indication. Also, it can be stated that certain temperature measurements can give acceptable SDS approximations if the measured temperature amplitude, during SDS sweep, is relatively narrow. In contrast, measuring the exhaust gas temperature of the IC engine, at the sections in front of and behind the turbine, in dynamic conditions, gives results that deviate significantly from stationary results, but these data could be used for further stationary test plan optimisation, such as optimizing of the stationary test plan execution order.

## REFERENCES

[1] Wiartalla, A.: "FEV study examines drivetrain topologies in 2030 - FEV," FEV Group GmbH, Aachen, Germany, Jul. 2017. Accessed: Apr. 23, 2019. [Online]. Available: http://magazine.fev.com/en/fev-study-examines-drivetrain-topologies-in-2030-2/.

[2] Krause, J., Thiel, C., Tsokolis, D., Samaras, Z., Rota, C., Ward, A., Prenninger, P., Coosemans, T., NeugebauerS., Verhoeve, W.: "EU road vehicle energy consumption and CO2 emissions by 2050 – Expert-based scenarios", Energy Policy, 2020, Vol. 138, p. 111224, Doi: 10.1016/j.enpol.2019.111224.

[3] Isermann, R.: "Engine Modeling and Control", Berlin, Heidelberg: Springer Berlin Heidelberg, 2014.

[4] Berger, B.: "Modeling and Optimization for Stationary Base Engine Calibration," Technische Universität München, Munich, Germany, 2012.

[5] Tietze, N.: "Model-based Calibration of Engine Control Units Using Gaussian Process Regression", PhD Thesis, Technische Universität, Darmstadt, 2015.

[6] Godburn, J., Brown, D., Case, R.: "Computer-controlled non-steady-state engine testing", International Journal of Vehicle Design, Vol. 12, No. 1, 1991, pp. 50–60. Doi: 10.1504/IJVD.1991.061671.

[7] Ward, M.C., Brace, C.J., Vaughan, N.D., Ceen, R., Hale, T., Kennedy, G.: "Investigation of 'Sweep' Mapping Approach on Engine Testbed", 2002. Doi: 10.4271/2002-01-0615.

[8] Keuth, N., Thomas, M., Pflügl, H., Martini, E., Bergold, S.: "Utilization of the Slow Dynamic Slope Methodology for the Calibration of the ECU-Functions 'Air Charge Determination' and 'Torque Prediction' in the Series Production," in Design of Experiments (DoE) in Engine Development: modern development methods to meet new challenges, Berlin, Germany, 2009, Vol. 1, pp. 122–136, [Online]. Available: http://d-nb.info/992518733.

[9] Leithgöb, R., Bollig, M., Büchel M., Henzinger F.: "Methodology for efficient calibration of model based ECU structures," Wiesbaden, 2005, pp. 195–210.

[10] Murakami, Y.: "Slow Dynamic Slopes (SDS) Methodology Applied for a Stratified Gasoline Engine," in Design of Experiments in Engine Development III, Renningen, Germany, 2007, pp. 413–423. [Online]. Available: http://d-nb.info/984171886.

[11] Mancini, G.: "Automotive Diesel Engine Transient Operation: Modeling, Optimization and Control," PhD Thesis, Università di Bologna, Bologna, 2014.

[12] Shimojo, K., Kitamura, Y., Sato, M., Adachi, S.: "Soot Modeling Using Quasi-Stationary Measurement for Gasoline Engine", Transactions of Society of Automotive Engineers of Japan, 2016, Vol. 47, No. 3, pp. 665–671. Doi: 10.11351/jsaeronbun.47.665.

[13] Miljić, N., Popović, S., Kitanović, M., Mrđa, P., Đinić, S., Petrović, V.: "Benchmarking of an existing engine in an automated way", AVL, Graz, Austria, ICED 1510/C01 SDS, Nov. 2015.

[14] Miljić, N., Popović, S., Mrđa, P., Kitanović, M. : "Slow Dynamic Slope method in IC engine benchmarking", Thermal Science, 2018, Vol. 22, No. 3, pp. 1271–1283. Doi: 10.2298/TSCI170921226M.

[15] Mrđa, P., Miljić, N., Popović, S., Kitanović, M.: "Continuous slow dynamic slope approach for stationary base internal combustion engine mapping", Thermal Science, 2020, Vol. 24, No. 1, pp. 147–158. Doi: 10.2298/TSCI190308171M.

[16] AVL List GmbH, "AVL CAMEO 4." AVL LIST GmbH Graz, 2018, [Online]. Available: https://www.avl.com/-/avl-cameo-4-.

[17] Nelles, O.: "Nonlinear System Identification, From Classical Approaches to Neural Networks and Fuzzy Models", Berlin, Heidelberg: Springer Berlin Heidelberg, 2001.

[18] Collette, Y.: "Planification d'expériences," Renault - Direction de la Recherche, 2006, [Online]. Available: http://ycollette.free.fr/Tools/Papers/Cours/01_Model_V3.pdf.

**MOBILITY & VEHICLE MECHANICS**

DOI: 10.24874/mvm.2021.47.03.04
**UDC: 62 833.6**

# HYBRID POWER TRAINS FOR HIGH-SPEED TRACKED VEHICLES

*Luka Ponorac[1]*, Aleksandar Grkić[2], Slavko Muždeka[3]*

*Received in July 2020* *Revised in September 2020* *Accepted in February 2021*

RESEARCH ARTICLE

**ABSTRACT:** Unlike independent steering systems on wheeled vehicles, the steering mechanism on high-speed tracked vehicles are integrated in the power train system, therefore turning process consumes more engine power than straight driving scenario. To ensure the most efficient turning performance, power trains of high speed tracked vehicles are equipped with complex turning mechanism components which are, most frequently, mechanical or hydrostatic. In most cases mechanical components enable turning process by slipping of the clutches and other frictional components, which is inconvenient from the aspect of power balance, as well as from the performance aspect. On the other hand, hydrostatic components have low efficiency in certain working ranges. Modernization of the conventional mechanical systems by applying electric drive components can contribute to solving the mentioned downsides, given the fact that modern electric drive systems can have very sensitive torque and speed regulation which significantly improves electric drive performance. Applying these electric drives in auxiliary power flow ensures additional flexibility and the possibility for the power train to work in different working regimes, such as energy regeneration, which improves the power train efficiency. This paper includes a variety of possible hybrid power trains for high-speed tracked combat vehicles and a fully developed simulation model of a hybrid drive for power trains with two power flows (main and auxiliary). The simulation model provides the possibility to observe the quantified influence of the certain parameter change in the turning process and allows us to identify the important parameters for power train control during the turning process.

**KEY WORDS**: hybrid power train, high-speed tracked vehicles, turning mechanisms, power train simulation model



[1]*Luka Ponorac, M.Sc.ME,inspection engineer, ADR laboratory, AMSS Motor Vehicle Centre Ltd, 58 Kneginje Zorke, 11000 Belgrade, Serbia, luka.ponorac@cmv.rs (*Corresponding author)*
[2]*Aleksandar Grkić, Head of ADR and ATP laboratories, AMSS Motor Vehicle Centre Ltd, 58 Kneginje Zorke, 11000 Belgrade, Serbia, aleksandargrkic@cmv.rs*
[3]*Slavko Muždeka, Assoc. prof., University of Defence in Belgrade, Military Academy, 33 Generala Pavla Jurišića Šturma Str., 11000 Belgrade, Serbia, slavko.muzdeka@gmail.com*

## HIBRIDNI SISTEM POGONA ZA BRZOHODA GUSENIČNA VOZILA

**REZIME**: Za razliku od nezavisnih sistema upravljanja na vozilima na točkovima, upravljački mehanizam na brzohodim guseničnim vozilima je integrisan u sistem pogona, pa proces zaokretanja vozila zahteva više snage od motora nego kod pravolinijske vožnje. Da bi se obezbedile najefikasnije performanse zaokretanja, pogonski sklopovi brzih vozila sa gusenicama opremljeni su složenim komponentama mehanizma za zaokretanje koje su najčešće mehaničke ili hidrostatičke. U većini slučajeva mehaničke komponente omogućavaju proces zaokretanja klizanjem spojnice i drugih frikcionih komponenata, što je nezgodno sa aspekta bilansa snage, kao i sa aspekta performansi. S druge strane, hidrostatičke komponente imaju nisku efikasnost u određenim radnim režimima. Modernizacija konvencionalnih mehaničkih sistema primenom komponenti električnog pogona može doprineti rešavanju pomenutih nedostataka, s obzirom na činjenicu da savremeni sistemi sa električnim pogonom mogu imati veoma osetljivu regulaciju obrtnog momenta i brzine koja značajno poboljšava performanse električnog pogona. Primena ovih električnih pogona u pomoćnom toku snage osigurava dodatnu fleksibilnost i mogućnost rada pogonskog sklopa u različitim režimima rada, poput regeneracije energije, što poboljšava efikasnost pogona. Ovaj rad uključuje niz mogućih hibridnih pogona za brza borbena vozila na gusenicama i potpuno razvijen simulacioni model hibridnog pogona za pogone sa dva toka snage (glavni i pomoćni). Simulacioni model pruža mogućnost posmatranja kvantifikovanog uticaja određene promene parametara u procesu okretanja i omogućava nam da identifikujemo važne parametre za upravljanje pogonom tokom procesa okretanja.

**KLJUČNE REČI**: hibridni pogon, brzohoda gusenična vozila, mehanizam zaokretanja, simulacioni model pogona

# HYBRID POWER TRAINS FOR HIGH-SPEED TRACKED VEHICLES

*Luka Ponorac, Aleksandar Grkić, Slavko Muždeka*

## INTRODUCTION

Since the development of electric motors as hybrid drives on commercial vehicles, there have been several attempts of applying the same technology on high-speed tracked vehicles, most commonly for military uses. The majority of these attempts are oriented on using electric motors as drive machines combined with IC engines. There are applications with parallel power flow [1], serial power flow [2], electric motors directly on drive wheels [3] etc. All of these solutions include using electric motors as drive machines and placing them in the main power flow, mainly to improve driving performances. On the other hand, these modernizations require electric motors with extremely high torque and power, as well as specific batteries and following electric systems which are usually very expensive. Modernization of the existing turning system integrated into the power train system presented in this paper represents a unique solution for manoeuvrability improvement. Applying electric motors in auxiliary drive, as turning mechanisms, provides significant improvement of turning parameters and potentially gives additional capabilities, while using non-expensive and relatively low power electric motors. Also, the capability to use electric motors as the source of drive power is maintained.

## 1. TURNING MECHANISM

Turning process of high-speed tracked vehicles is much more complex than wheeled vehicle turning process. Unlike with wheeled vehicle steering systems, tracked vehicles require significantly more engine power/torque for turning, than for linear movement. This is because of the high levels of force that resists the turning of the vehicle, which are not present during linear movement, or are present on a much lower level. Figure 1 shows the simplified mechanical model of the tracked vehicle during the turning process [4].

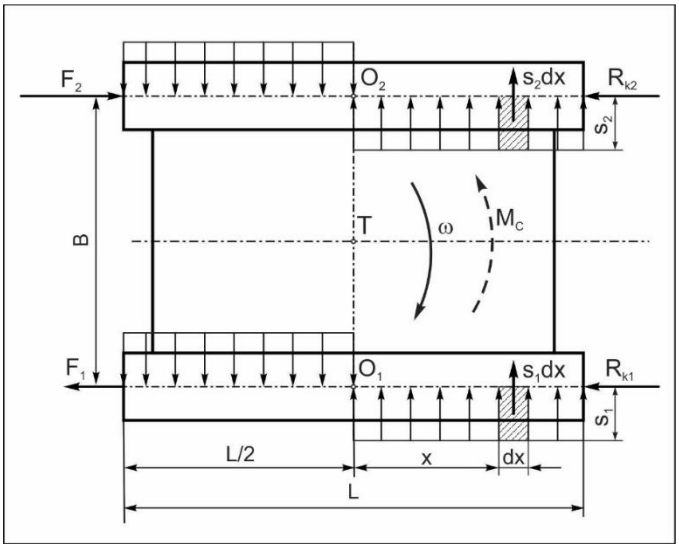


*Figure 1 Resisting forces during the turning process*

where:

- $R_{k1}, R_{k2}$ [N] – lienear movement ressistance
- $s_1, s_2$ [Nm] -specific ressistance to transversal track movement

$F_1, F_2$ [N]-braking force on the inner/drive force on the outer track.

Turning mechanisms on tracked vehicles provide the rotational speed difference between left and right drive wheel, that is, winding speed difference between inner and outer track, thus enabling the tracked vehicle to make a turn. The main parameter that describes the turning process is turning radius. As mentioned, turning process is achieved by enabling the winding speed difference of the tracks, which means that the turning radius is defined by the translational speed of the inner and outer track. This relation comes from the kinematic analyses of the tracked vehicle turning process and is described by the following equation:

$$R = \frac{B}{2} \cdot \frac{V_2 + V_1}{V_2 - V}, \tag{1}$$

where:

- $B$ -track width
- $V_2, V_1$ -translational velocities of outer and inner track

Generally, there are two types of turning mechanisms applied in high-speed tracked vehicle:

- Symmetrical/differential
- Asymmetrical.

During the turning process, the symmetrical turning mechanism allows the vehicle mass centre to keep the velocity that it had during the linear movement. Most commonly, the outer track gains velocity for the same value that the inner track velocity is reduced, comparing to mass centre. This allows the vehicle the advantage of pivot turn, around its own vertical axis. The downside of these turning mechanisms is their construction complexity; most commonly combined with hydrostatic and additional mechanical components (“zero” shaft). During the turning process, the asymmetrical turning mechanism ensures that one point on the vehicle, usually the outer track, keeps the velocity of the linear movement, while the velocity of the mass centre and inner track is reduced.

## 2. BVP M80A POWER TRAIN CONSTRUCTION

The power train analysed in this paper is the power train of the infantry fighting vehicle BVP M80A, with an asymmetrical turning mechanism. It is a mechanical, integrated power train, with parallel main and auxiliary power flow. The main power flow is achieved through the mechanical gearbox (labelled as MP, Figure 2) and joins with the auxiliary power flow in the turning mechanism, that is, in the planetary gear set. Vehicle power train scheme is shown in Figure 2.

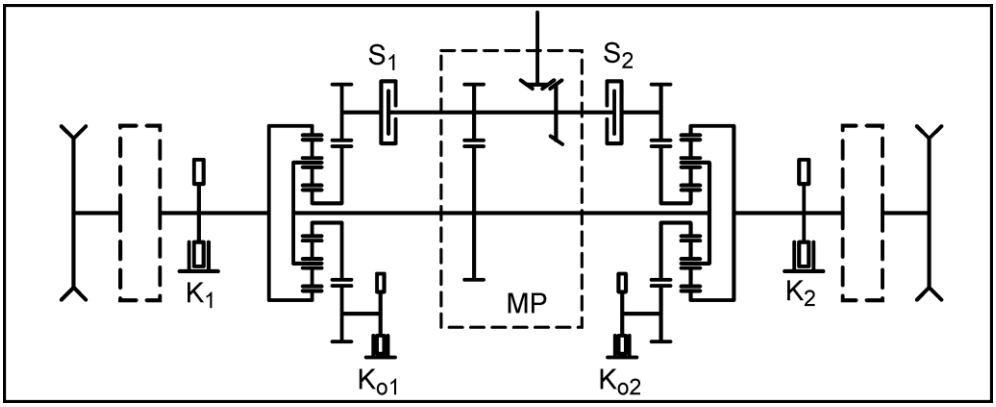


*Figure 2 Turning mechanism scheme*

The angular velocity on both planet carriers, which are connected to the gearbox output shaft, are the same. The difference in angular velocity on ring gears, thus on drive wheels, is achieved with sun gears, which are connected to the auxiliary power flow. During the linear movement, the sun gears are braked by brakes and . When the turning process starts one of the mentioned brakes is disengaged, while the engagement of clutch or gradually starts. When one of the clutches is engaged, the corresponding sun gear speeds up, thus reducing the angular velocity of the ring gear and the drive wheel. The described turning mechanism achieves the requested turning radius by slipping of the friction elements for all turning radii except for those when the friction elements are fully engaged. When the friction elements of the turning mechanism are fully engaged, the turning radii achieved in these states are called calculated turning radii, and for this type of turning mechanism, there are two turning.

The first one is achieved when the clutch ( $S_1$ or $S_2$ ) on the inner track sun gear is engaged, while the sun gear on the other side is braked.

The second calculated radius is achieved when the power train output shaft/drive wheel is braked with brakes $K_1$ or $K_2$ , so the vehicle turns around the inner track.

There is a specific state where none of the friction elements on the inner track part of the power train are engaged, so there is neither drive nor braking force on the inner track, thus allowing the track to wind freely.

Worn surfaces of the shoe sleeve were measured in two planes and two mutually perpendicular sections. The location of the planes: A – A - 15 mm from the end face of the sleeve B – B -. 10 mm from the flange of the sleeve. The measurement scheme is shown in Figure 3.

*D* – bushing outer diameter; *d* – bushing inner diameter; $d_1$ – diameter of inner worn surface; *L* – amount of wear.

The measurement of the inner diameter is carried out using the indicator caliper IC 10 GOST 868 - 82 with a division value of 0.01 mm (Figure 4).

## 3. PROPOSED MODERNIZATION

The previously described turning system has many drawbacks. Having the defined number of turning radii can be a downside, especially because not all of them can be achieved in every driving condition. Because of the abrupt changes of the turning states, it is common that the driver makes a mistake and doesn't anticipate the turning conditions, which can lead to the track falling of the drive wheel, vehicle instability and similar inconveniences. One of the possible solutions for overcoming the stated problems is applying electric motors in the auxiliary drive, instead of clutches and (Figure 2). This means that the auxiliary drive power would no longer be drawn from the IC engine, but from the electric motors instead, making the auxiliary drive independent. Figures 3a and 3b show the potential placement of the electric motors (EM) in the auxiliary drive.

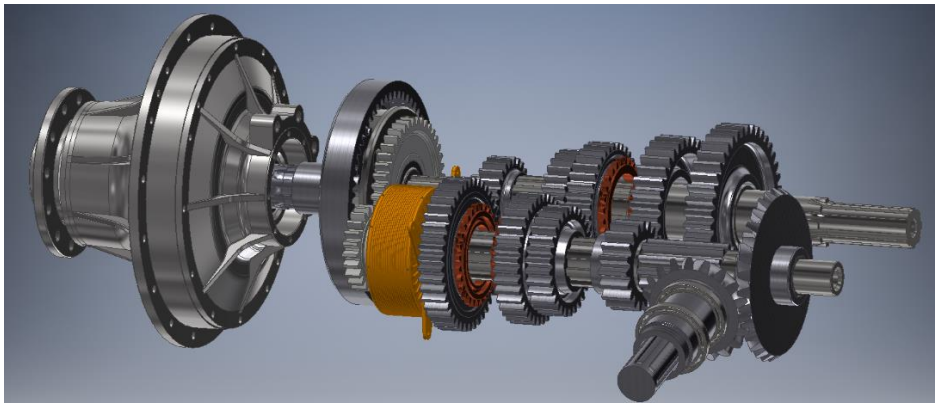

*Figure 3a Electric motor in auxiliary drive (power train left cross section)*

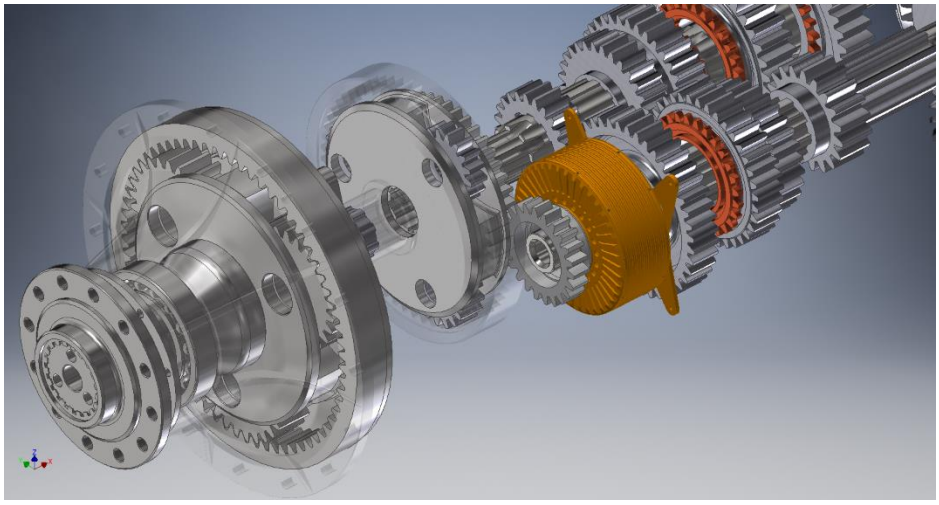

*Figure 3b Electric motor in auxiliary drive (power train left cross section*

Precise speed control of the electric motors would result with achieving the wanted sun gear angular speed, thus being able to control the speed of the inner track. As a result, in a certain range, there would potentially be an infinite number of turning radii, and the turning process would be smoother. Applying electric motors in the auxiliary drive eliminates the losses of

the turning mechanism friction components, and the torque characteristic of the electric engine, which is maximum at motor start, is compatible to the requirements of the turning dynamics. One of the important improvements of this conception is that it allows the power train and turning mechanisms to act as both symmetric and asymmetric. If the electric motor of the outer track is braked, and the one on the inner brake is working, the turning mechanisms will act as asymmetric. On the other hand, if the electric motor of the inner track is reducing its speed for a certain value, and the other motor enables the speed increase of the outer track for the same value, the turning mechanisms would act as symmetric. As a result, the vehicle would be able to make a pivot turn. There are other perks of applying electric motors in the auxiliary drive such as driving only on electric power, generating power in certain turning states etc. When it comes to cost and energy effectiveness, the electric auxiliary drive could potentially be carried out with minimum expenses and reconstruction of the existing power train. If synchronous electric motors were applied on the subject vehicle, instead of the previously described turning mechanism clutches, they need not have the power greater than $P = 50$ kW and angular velocity not greater than $n = 2000$ rpm. As for the batteries and power grid, the system works on nominal voltage of $U = 460$ V and amperage of $I = 200$ A.

## 4. SIMULATION MODEL

For the purpose of comparative analyses of turning mechanism performance, simulation models were developed for both existing mechanical and proposed hybrid power train. The simulation models allow us to run kinematic and dynamic analyses for both power trains and acquire data needed for comparative analyses, such as track velocity, torque, turning radius, engine load, as well as to determine required parameters for the hybrid power train auxiliary drive. Since the difference between the existing and proposed power train is in the auxiliary drive, the existing power train simulation model will be described fully, while only describing the difference of the hybrid power train simulation model. The BVP M80A simulation model consists of three subsystems/groups of mechanical components (Figure 4):

- IC engine with main friction clutch
- Integrated power train subsystem
- Track subsystem.

Other than these mechanical component groups, there are:

- Control signals
- Results.

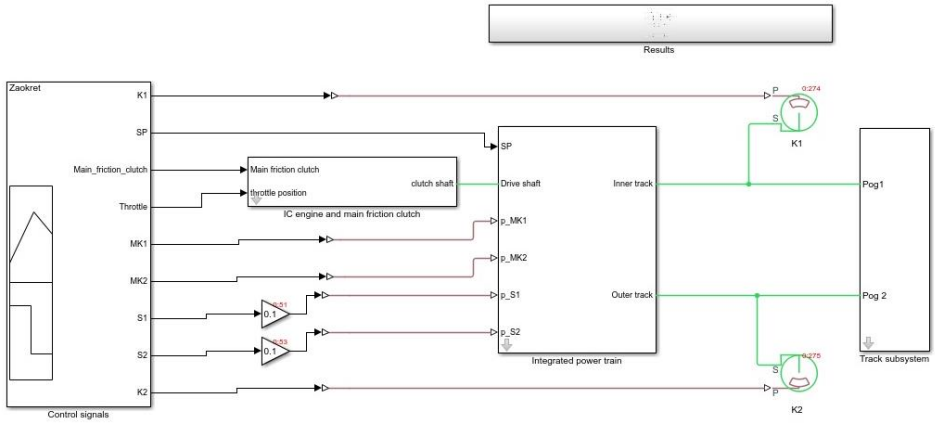


*Figure 4 Vehicle simulation model*

### *4.1 IC engine and main friction clutch subsystem*

The IC engine with main friction clutch subsystem consists of engine block and main friction clutch block with activation command and lever system (Figure 5). This subsystem provides the drive power parameters (torque and angular velocity) and transfers them to the power train. The IC engine is conducted by the throttle position signal, and the clutch is engaged/disengaged by the activation force signal, both from the control signal block.

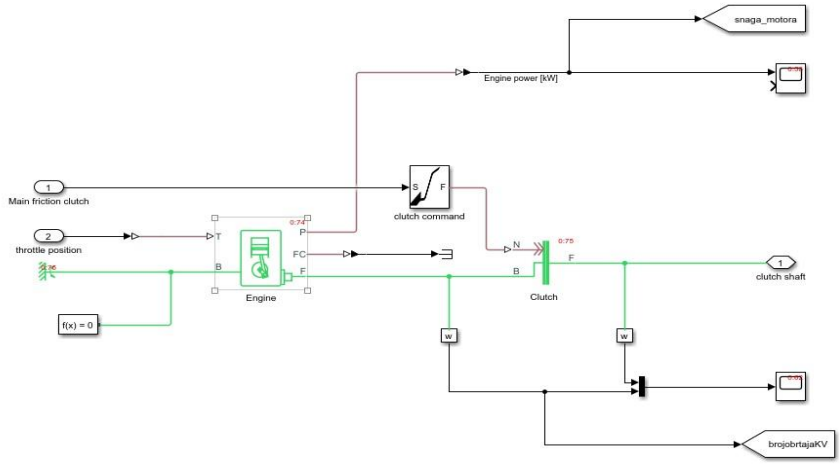


*Figure 5 Engine and main friction clutch block*

### *4.2 Integrated power train subsystem*

Integrated power train subsystem consists of mechanical gearbox components and turning mechanism components (Figure 6) and has the role of transferring and altering torque and angular velocity, as well as enabling the turning process of the vehicle through the auxiliary drive.

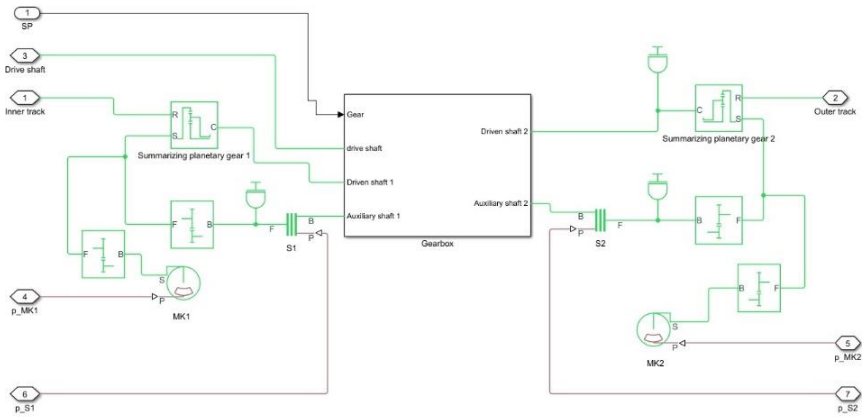


*Figure 6* Integrated power train block

The mechanical gearbox (Figure 7) is driven by the main friction clutch shaft. It has five forward gears and one reverse gear, all of them engaged with synchronizers. The power is transferred from the drive shaft to the driven shaft via transfer shaft. The gear changing is achieved by sending gear request signal, from the control signal block, too a multi-position switch. The switch sends the activation signal to the gear actuators where the actuation force is generated and transferred to the corresponding synchronizers via lever system, thus activating the requested gear.

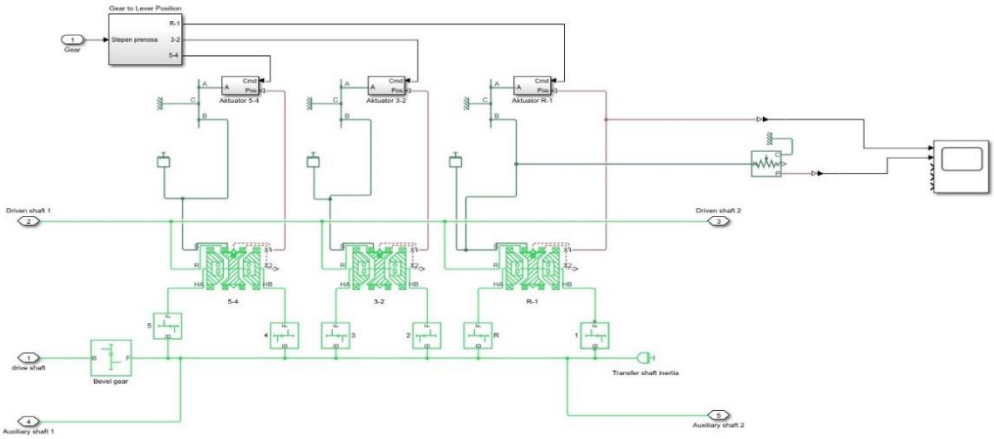


*Figure 7 Mechanical gearbox block*

The driven shaft has two exit points, for left and right track systems. The driven shaft transfers power to the planet carrier of the summarizing planetary gears. The transfer shaft of the gearbox is also the auxiliary drive shaft. When turning, the auxiliary drive shaft is connected to the sun gear of one of the summarizing planetary gears via friction clutches S1 or S2. When moving forward, the sun gear is braked by disc brakes MK1 or MK2 (Figure 6). The ring gear of both summarizing planetary gear sets are connected to the integrated power train exit shaft and transfer the drive power to the sprocket and track subsystem.

### *4.3 Sprocket and track subsystem*

Sprocket and track subsystem represents the components which come after the integrated power train in the kinematic chain, as well as the resisting forces on the tracks (Figure 8). It consists of the inner and outer (left and right) track subsystems, turning radius calculus subsystem and components for different measurement display.

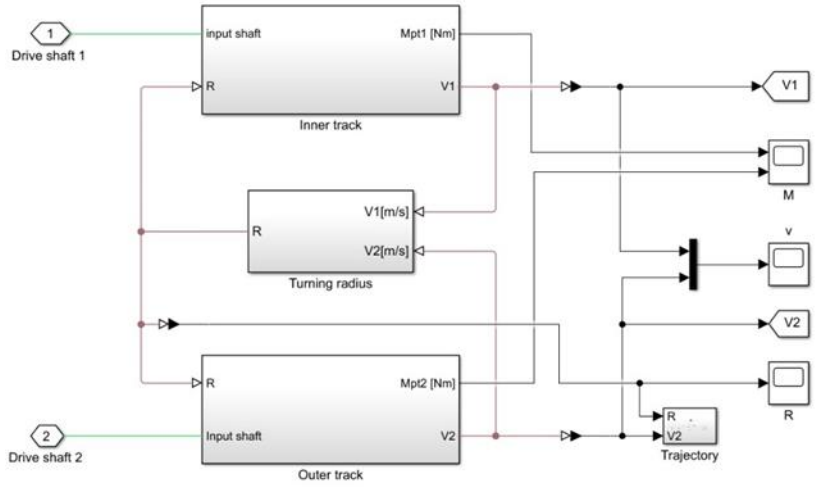


*Figure 8 Sprocket and track subsystem*

The inner and outer track subsystem consists of mechanical components representing the real elements of the power train, and the physical signals which simulate the moving resisting forces on tracks (Figure 9). These physical signals are connected to a torque source, thus becoming a real load on the mechanical power train components. The summarizing load on the mechanical components is measured and it represents the sprocket/drive wheel torque. By measuring the angular velocity of the mechanical components, we acquire the information about translational track velocity, which figures in the turning radius and turning resistance calculus.

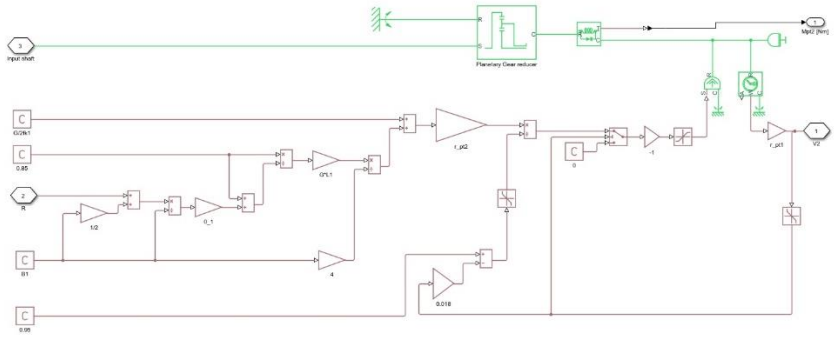

*Figure 9 Track subsystem*

### *4.4 Elecrtic auxiliary drive*

As mentioned, the main difference between the existing and modernized vehicle power train is in the auxiliary drive (Figure 10). The auxiliary drive of the modernized power train consists of two electric motors applied instead of friction clutches S1 and S2. The electric motors are represented with two asynchronous electric motor blocks labeled MG1 and MG2 (Figure 11). The electric motors have a mechanical connection with the sun gears of the summarizing planetary gear sets, electrical connection with the batteries and connections concerning the acquisition of measured values.

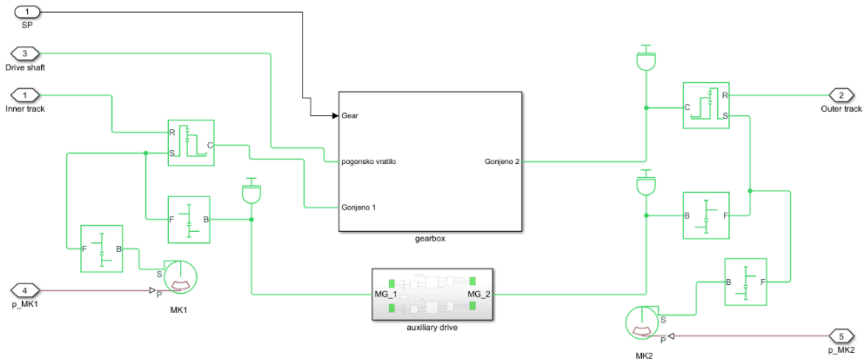


*Figure 10 Electric integrated power train*

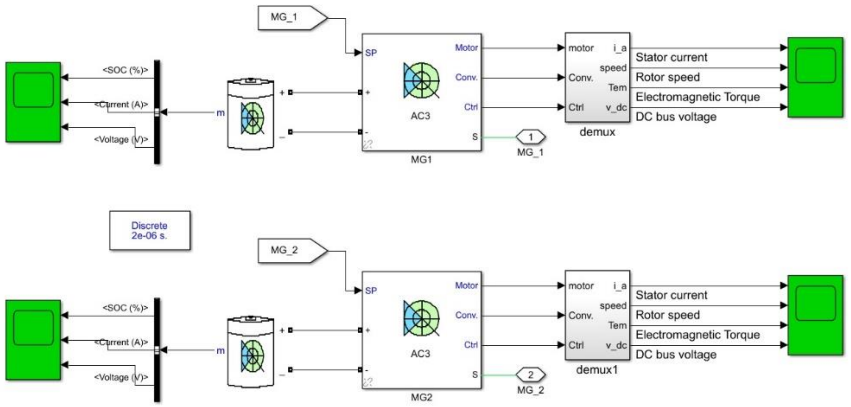


*Figure 11 Electric auxiliary drive subsystem*

The electric motors are controled with the signal from the control signal block. The signal represents the requested value for motor angular velocity (rpm). The motors are still in forward movement (except for the case when they are both working and driving the vehicle only with electric energy). When turning, the motor of the inner track speeds up the sun gear of the summarizing planetary gear set. Given the fact that the batteries give direct current, and the motors work on alternated current, the MG1 and MG2 motor blocks contain inverters and other necessery components for the DC/AC conversion. The battery model is based on experimental validation [5].

## 5. SIMULATION MODEL ANALYSES

To evaluate the quality of the turning mechanism hybridization, a simulation of the turning process is made, with the same conditions, for both mechanical and hybrid turning mechanisms. The simulation scenario implies the vehicle movement starting from the still state in first gear and turning with the parameters which will result with the same values of velocity and turning radius, at the end of the turning process. The analisys of the mechanical power train implies graduatelly deacivating Ko1 brake, followed by engaging the S1 friction clutch. As for the hybrid turning mechanism, the equivalent state would be engaging the inner track electric motor to the angular velocity coresponding the angular velocity of the auxiliary drive of the mechanical turning mechanism. Figure 12. shows the outer track velocity (v2), inner track velocity (v1) and center of mass velocity (v), where the values labeled MD refer to mechanical drive, while the ones labeled HD refer to hybrid drive. It is apparent that the inner track velocity change of the mechanical turning mechanism is faster than in the case of hybrid drive, which is a consequence of the incapability of precise slip regulation of friction elements. This happens in practice as well, which is why tracked vehicles with mechanical turning mechanisms can't achieve continuous turning. On the other hand, it is clear that the hybrid turning mechanism has a more mild and continuous velocity change.

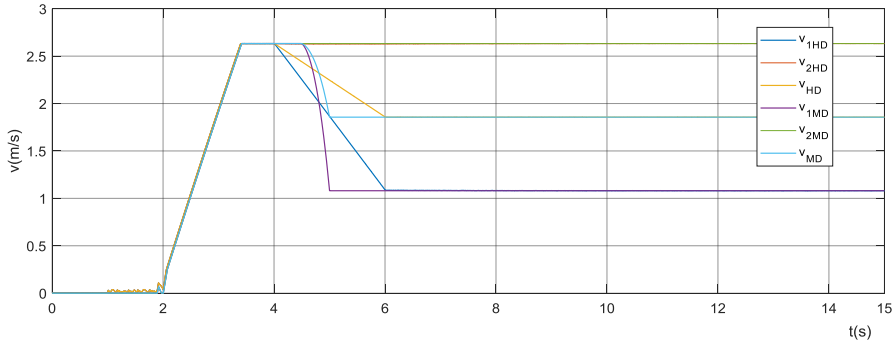


*Figure 12 Track velocities during the turning process*

Above mentioned is obvious in turning radius analysis as well, where we can observe that with the hybrid turning mechanism the requested turning radius is achieved continuous, unlike with the mechanical turning mechanism, where the requested turning radius is achived faster, but with greater dynamic loads on the power train elements.

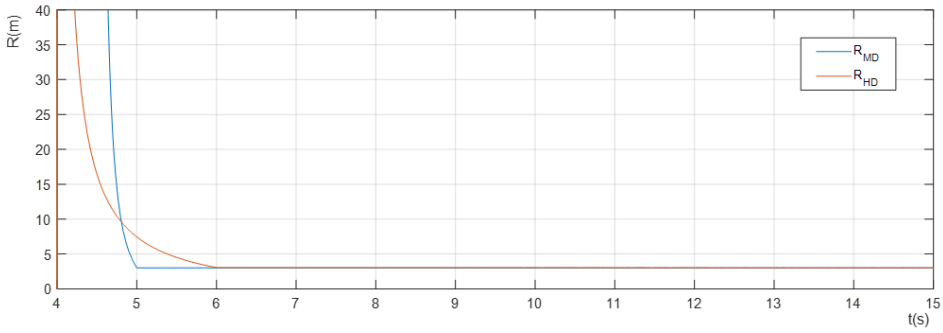


*Figure 13 Turning radius change*

The power of the drive units during the turning process is shown in Figure 14. It is clear that, in stationary regimes, with both types of turning mechanisms, the total power of the power train is equivalent, which is expected concerning the fact that the turning process with mechanical turning mechanism is achieved without slipping losses of the friction elements. However, it is also obvious that during the turning process of the hybrid turning mechanism, significantly less power of the ICE engine (P_ICE) is being consumed for the turning process, which is important from the aspect of the vehicle performance improvement with this type of hybridization. It is important to state that the quality of the hybrid turning mechanism is shown at state of turning radius different than calculated turning radii, which is a most common state during the turning process, when it is expected that the total power of the power train is less than the requested drive unit power of the power train with the mechanical turning mechanism. Also, the hybrid turning mechanism can ensure any turning radius with a stable and requested value.

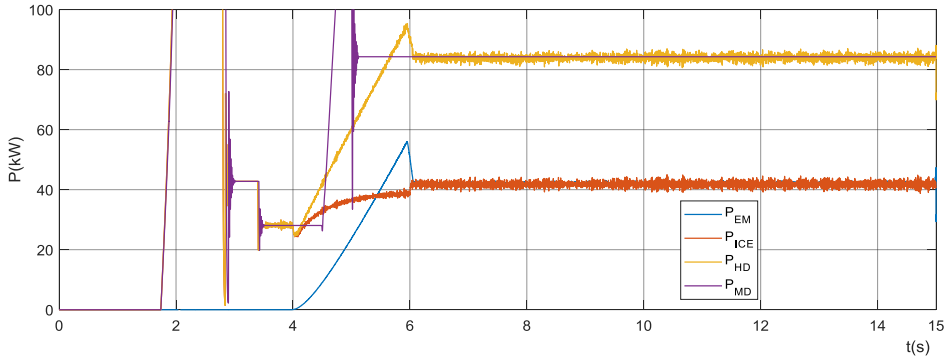


*Figure 14 Power change of the drive units during turning process*

## 6. CONCLUSIONS

The development of the electric drive technologies has given us the possibility to draw significant power parameters from compact and simple electric motors with reasonable energy consumption. Implementing these drives in tracked vehicles allows us to make noticeable improvements of the vehicle performance, energy consumption and manipulation. Most important power train improvements with hybrid turning mechanisms is ensuring continuous and stable turning process, with significantly less IC engine power consumed. The turning process is fully controlled and infinite number of turning radii, within a given range, can be achieved and maintained. Also, there is an aspect of energy generation by electric motors, in certain driving states, which were not considered in this paper. However, the drawbacks of these solutions should be considered as well. Power trains with electric motors require large storages of electric energy, which have to provide enough electric energy for turning processes in hard condition, repeatedly. These electric motors have variable efficiency, making them inefficient in certain regimes. There is a difficulty of physical placement and cooling of the electric components in the confined space such as the housing of the integrated power train of the considered track vehicle. On the other hand, power train with mechanical turning mechanism do not require batteries and other expensive electric components, but they draw a significant amount of IC engine power for turning, decreasing the vehicle performance parameters, turning process is mostly unstable and intermittent, with intensive loads on the friction and other power train

elements. There are also noticeable inefficiencies in the turning mechanism from the friction elements slip losses, which are not especially shown in this paper, but have a negative impact on the vehicle turning process.

## REFERENCES

[1] Sivakumar, P., Rajaseeli, R., Venkatesan, G., Viswanath, H., Selvathai, T.: "Configuration Study of Hybrid Electric Power Pack for Tracked Combat Vehicles", Defence Science Journal, 2017, Vol. 67, No. 4, pp. 354-359. Doi: 10.14429/dsj.67.11454.

[2] Ilijevski, Ž.: "A Hybrid-Electric Drive Concept for High Speed Tracked Vehicles", Proceedings of the 13th International ISTVS Conference, 2003, Munich, Germany.

[3] Bhatia, V.: "Hybrid tracked combat vehicle", 2015 IEEE International Transportation Electrification Conference (ITEC), Chennai, 27-29 August 2015, pp. 1-23. Doi: 10.1109/ITEC-INDIA.2015.7386862.

[4] Muždeka, S., Pantić, M., Arsenić, Ž.: "Vučne performanse zaokreta brzohodnih guseničnih vozila", Međunarodni simpozijum (13) MVM, Kragujevac, 2004. (in Serbian).

[5] Tremblay, O., Dessaint, L.A.: "Experimental Validation of a Battery Dynamic Model for EV Applications", World Electric Vehicle Journal, 2009, Vol. 3, Iss. 2, pp. 289-298. Doi: 10.3390/wevj3020289.

**MOBILITY & VEHICLE MECHANICS**

DOI: 10.24874/mvm.2021.47.03.05
**UDC: 620.193.95**

# THE EFFECT OF CORROSION ON A STRUCTURAL INTEGRITY AND VEHICLE SAFETY

*Valentina Golubović-Bugarski[1]*, Snežana Petković[2], Gordana Globočki-Lakić[3]*

*Received in July 2020* *Revised in August 2020* *Accepted in March 2021*

RESEARCH ARTICLE

**ABSTRACT:** The problem of corrosion is a problem of global importance, and significant attention has been paid to this problem during last years. On the one hand, the effect of corrosion on a vehicle depends on how excessively the corrosion has spread to the structural element and, on the other hand, depends on the specific function of structural element where corrosion is found. Thus, safety of the vehicle might be significantly reduced if the corrosion spreads on the vital structural component of the vehicle. Even a small amount of corrosion that disrupts the continuity of the load bearing structure, can endanger the bearing capacity of a given structural component. A special problem from the aspect of safety is the corrosion of the vehicle frame (chassis). This paper presents an analysis of the effects of weakening of the frame due to corrosion on the predicted design bearing characteristics and safety operation parameters, which the vehicle possesses at the beginning of its service life. By reducing the dimensions of the vehicle frame due to corrosion, critical areas of the structure will ocurre, to which an additional attention should be paid during the design and control of the frame condition. The analysis was performed using the Solidworks Static Simulation program. Regarding that the occurrence of corrosion can weaken the load bearing structural elements and reduce the safety of the vehicle, it is necessary to improve the technical inspections of the vehicle and periodically check the condition of the vehicle in terms of corrosion and structural integrity.

**KEY WORDS**: vehicle corrosion, structural integrity, vehicle safety, technical inspection



[1]*Valentina Golubović Bugarski, University of Banja Luka, Faculty of Mechanical Engineering, Banja Luka, valentina.golubovic-bugarski@mf.unibl.org (*Corresponding author)*
[2]*Snežana Petković, University of Banja Luka, Faculty of Mechanical Engineering,Banja Luka snezana.petkovic@mf.unibl.org*
[3]*Gordana Globočki Lakić, University of Banja Luka, Faculty of Mechanical Engineering, Banja Luka, gordana.globocki-lakic@mf.unibl.org*

## UTICAJ KOROZIJE NA INTEGRITET STRUKTURE I SIGURNOST VOZILA

**REZIME**: Problem korozije je problem od globalnog značaja, a poslednjih godina ovom problemu je posvećena značajna pažnja. S jedne strane, uticaj korozije na vozilo zavisi od toga koliko se korozija prekomerno proširila na element konstrukcije, a sa druge strane zavisi od specifične funkcije strukturnog elementa na kome se nalazi korozija. Stoga bi se sigurnost vozila mogla značajno smanjiti ako se korozija proširi na vitalnu konstrukcijsku komponentu vozila. Čak i mala korozije koja narušava kontinuitet nosive konstrukcije, može ugroziti nosivost date komponente konstrukcije. Poseban problem sa aspekta bezbednosti predstavlja korozija okvira vozila (šasije). U ovom radu je prikazana analiza uticaja slabljenja okvira usled korozije na predviđene projektne karakteristike ležaja i bezbednosne radne parametre, koje vozilo poseduje na početku svog radnog veka. Smanjenjem dimenzija okvira vozila zbog korozije, pojaviće se kritična područja konstrukcije, na šta treba obratiti dodatnu pažnju prilikom projektovanja i kontrole stanja okvira. Analiza je izvršena korišćenjem programa Solidworks Static Simulation. S obzirom da pojava korozije može oslabiti nosive konstrukcijske elemente i smanjiti sigurnost vozila, potrebno je poboljšati tehničke preglede vozila i povremeno proveravati stanje vozila u pogledu korozije i celovitosti konstrukcije.

**KLJUČNE REČI**: korozija vozila, integritet strukture, bezbednost vozila, tehnički pregled

# THE EFFECT OF CORROSION ON A STRUCTURAL INTEGRITY AND VEHICLE SAFETY

*Valentina Golubović-Bugarski, Snežana Petković, Gordana Globočki-Lakić*

## INTRODUCTION

Corrosion that occurs on vehicles is a problem that endangers traffic safety and has an adverse financial effect on the economy of any country. Until the late 1950s, corrosion of motor vehicles was considered to be a problem that occurs exclusively in marine and coastal environments. However, in the following years, a large number of vehicles used within the continent areas were shown to corrode and become unusable in just a few years, and the reason for that was found in the intensive use of salt as protection against road icing in the winter [2]. Motor vehicles produced during the last decades have very little visible corrosion thanks to numerous technological improvements introduced in the process of vehicle design and production. However, the annual costs related to corrosion are still significant and still much can be done to reduce them. In 2002, the US Federal Highway Administration released a study [5] on the direct costs associated with metallic corrosion in the US industry. In 1998, the total annual direct cost of corrosion in the U.S. was ca. $276 billion (ca. 3.2% of the US gross domestic product). Broken down into five specific industries the economic losses are $22.6 billion in infrastructure; $17.6 billion in production and manufacturing; $29.7 billion in transportation; $20.1 billion in government; and $47.9 billion in utilities. Corrosion is the natural process of gradual destruction of materials (usually a metal) by chemical and/or electrochemical reaction with environment in which the material is located. It causes measurable material changes and leads to corrosion damage. It is formed on the surface of the metal and spreads faster or slower from the surface to the depth, whereby the chemical composition and properties of the metal change. It occurs as a consequence of physical - chemical processes: a) when metal is in contact with an aggressive environment (metal - water, metal - acid, metal - air, metal - earth, etc.), b) in contact of dissimilar metals and c) on the contact surface of two metal grains with different composition or different voltage state. In the process of corrosion, the metal completely or partially dissolves or a precipitate forms on the metal surface (rust formed during corrosion of iron in a humid environment). Due to corrosion, in some cases the alloys decompose into components or the physical - chemical properties of metals and alloys change. Corrosion degrades the useful properties of materials and structures including strength, appearance and permeability to liquids and gases. The corrosion reaction can be represented in a simple way by the relation [3]: *metal + environment = corrosive product.*

## 1. TURNING MECHANISM

According to the domination, corrosion can be uniform - over the entire surface of the metal product and local - only on certain metal surfaces. The most common type of corrosion of metal parts is uniform corrosion. It is present over the entire surface of a metal object which is in a contact with an aggressive environment. In the case of local corrosion, only certain parts of the surface of the material are subject to destruction. Corrosion can be concentrated locally to form a pit or crack. It is so-called pitting which causes destruction of individual zones and is unevenly distributed over the surface. Characteristic of pitting corrosion is the appearance of holes that penetrate into the depth of metal parts. In cases when the contact of metals of different electrical potential is dominant in the presence of electrolytes, contact (galvanic) corrosion will occur.

The most unfavorable form of corrosion is intergranular corrosion because it occurs at the boundaries of metal grains and penetrates very quickly and deeply into the metal. Due to corrosion, the bond of crystal grains weakens, and thus the metal parts losing its strength. There is corrosion without mechanical load and corrosion under mechanical load. Corrosion without mechanical load is divided into two subgroups, depending on the physical state. The first is corrosion in the watery medium (contact, pitting and corrosion in the gaps), and the second - corrosion in the gaseous medium (chemically induced hydrogen occurrence, oxidation and formation of deposits). Corrosion under mechanical load in the watery medium refers to stress corrosion, corrosive fatigue, erosion corrosion. In order to any of these corrosion be initiated, it is necessary that, in addition to the material and the working environment, an external load also participates, where cracks can occure as a consequence of the action of the load. In most cases, the corrosion reaction is of electrochemical character, and it can also occur due to the action of chemical and physical processes. Thus, according to the reaction mechanism, one can distinguish two types of corrosion - chemical and electrochemical. Chemical corrosion is caused by the interaction of metals and gases at raised temperatures (gas corrosion), and electrochemical - by the action of electrolytes on the metal, which is the most common form of corrosion.

### *1.1 Electrochemical corrosion*

Most metal structures are in contact with air, which also contains water vapor, carbonic acid, sulfur-based gases and other impurities that dissolve in moisture droplets. The surface of such exposed structures is covered with moisture, saturated salts, bases, acids, or a layer of electrolyte that directly participates in the process of electrochemical corrosion of metals. It is based on the ability of the metal to ionize (release electrons) and the corresponding medium (electrolyte). The measure of this phenomenon is the electrode potential, which is defined as the difference between the potential of a metal and the so-called standard (reference) hydrogen electrodes, whose potential is zero. Metals with a higher ability to release electrons have a negative electrode potential, so they are considered as a cathode. Metals, especially alloys, are inhomogeneous in structure and chemical composition (solid solutions of eutectic mixtures and chemical compounds have different electrode potentials). When some alloys are immersed in an electrolyte, some of its areas have a lower electrode potential, become anode and are destroyed, while other areas of the alloy with a higher potential, as a cathode, remain unchanged. Since there are many such anode and cathode regions, it is considered that the alloy consists of a large number of anodes and cathodes. Metal or alloy joints can also have an increased tendency to corrosion (for example, a joint between a sheet made of aluminum alloy - anode and a brass screw - cathode, where the sheet is subject to corrosion destruction) [7].

## 2. METAL CORROSION IN AUTOMOTIVE PARTS

Corrosion on motor vehicles occurs in several forms. Characteristic vehicle areas affected by corrosion are: bearing elements, exhaust system, braking system, driving system, cooling system parts, engine parts (pistons and cylinders). General corrosion is the most common type of corrosion on vehicles that occurs on the outer metal panels of the vehicle body and chassis, Figure 1a. The result of such corrosion is occurence of surface damage, which impairs the appearance of the vehicle and prevents the proper operation of the vehicle, due to which the vehicle loses its resale value. General corrosion also affects the underside of the vehicle and the vehicle frame, which can lead to surface damage to the floor plate and weakening of the frame. The most common type of general corrosion on a vehicle is uneven general corrosion. It affects individual parts and vehicle areas that are located in zones

suitable for its acting. Pitting occurs when the metal parts come into contact with chlorides and other chemical species. This can cause a corrosive reaction locally producing small cavities. Due to the existence of these small cavities, there is a leak in the radiator and in the muffler and tail pipe (pitting inside tail pipe is shown in the Figure 1b). Corrosion inhibitors are added to the coolant to prevent corrosion of the cooling system.

*Figure 1 Forms of vehicle corrosion: a) general corrosion of vehicle body panels, b) pitting in the tail pipe, c) Contact corrosion between two different metals*

Galvanic (contact) corrosion occurs when different metals are in contact, where one of the metals is more electrochemically active and corrodes, while the other metal is protected by this corroded metal, Figure 1c. Galvanic corrosion was considered more as a cosmetic damage and disadvantage at a time when more metals were combined for decoration of vehicles (nowadays, this is no longer the case). The occurrence of galvanic corrosion can be significantly reduced by the correct design of the vehicle, but its action must certainly be borne in mind when different materials are used in the construction of the vehicle. Corrosion in gaps (crevice) occurs when fluid penetrates into narrow gaps between two surfaces, e.g. between a steel support and washer on a windshield wiper, etc. The fluid can concentrate in a narrow gap causing severe corrosion.

### *2.1 Causes of corrosion on vehicles*

There are several factors that affect the occurrence of corrosion on vehicles, which are related to the process of vehicle design, the production process and the working conditions themselves [4].

#### 2.1.1 Vehicle design

It happens that in the process of a vehicle design, a wrong design solution is adopted sometimes, which can be the reason that corrosion appears on vehicle in use. Therefore, some design requirements for corrosion protection should be met at the vehicle design stage. Namely, it is necessary to avoid direct contact between metals that have different corrosion potential, to avoid designing cracks and gaps in which fluids, salt and road impurities can accumulate. The choice of material during vehicle design can also significantly affect the later occurrence of corrosion. In order for the vehicle to be in use for as long as possible without corrosion, it is necessary to use corrosion-resistant metals, apply appropriate surface protection of materials, use polymers, and it is also important to avoid direct contact of different metals. One of the key decisions to be made in the vehicle design phase is the choice of protective paints, varnishes and impermeable coatings. Therefore, nowadays in the automotive industry, it has become the standard to apply protective paints to the entire body of the vehicle, to treat fenders and lower surfaces with special coatings that protect surfaces from impact damage, to minimize the initial occurrence of corrosion.

#### 2.1.2 Production process

It can happen that a good choice of design solutions adopted in the vehicle design phase is almost annulled due to the low quality of production. There are several elements of the production process that are especially important from the point of view of vehicle corrosion protection. First, the quality of the welding can affect the appearance of cracks in which corrosion can be initiated. Then, the preliminary preparation of the surfaces should be performed in an appropriate way to ensure a good adhesion of the primer and finishing coatings. Finally, some specific protections such as impact-resistant coatings and sealing coatings can be applied by hand, so that their quality largely depends on the expertise and skill of the workers.

#### 2.1.3 Vehicle operating conditions

The characteristics of the environment and atmospheric conditions characteristic for the region where the vehicle is used, such as acid rain, the use of deicing salt in the winter, the influence of the sea climate, strongly influence the occurrence of corrosion on vehicles. In such corrosive environments, the personal habits of the vehicle owner and good maintenance of the vehicle (regular washing, fluid change) come to the fore, which can significantly increase the vehicle's resistance to corrosion.

## 3. IMPACT OF CORROSION ON VEHICLE SAFETY

On the one hand, the impact of corrosion on the safety of vehicle depends on how much the corrosion has spread, and on the other hand, on the function of the structural element that has been corroded. If corrosion has affected a vital structural part of the vehicle, the safety of the vehicle can be endangered even by the appearance of a small amount of corrosion which affects the continuity of the supporting structure, i.e. endangers the load bearing capacity of the structural component. On the other hand, if the corrosion has excessive affected some parts of the vehicle that do not have a load-bearing significance, in that case the corrosion has little or almost no impact on the safety of the vehicle. Corrosion of some specific parts, e.g. door sills, can be very important for one type of vehicle construction, while for another type of construction it may not be significant. Figure 2 shows the structural elements of a passenger vehicle, where the shaded portions indicate the important load bearing parts of various typical vehicle constructions [6]. Certain areas of the vehicle structure are particularly important for the vehicle safety. These areas are:

- Load bearing parts of the vehicle to which other parts of the vehicle are mounted, specially parts that are subject to technical inspection (steering parts, levers and suspension joints, shock absorbers, braking system, seat belts, fenders, bumpers, additional safety systems).
- Any other load bearing or supporting elements or supporting panelling located up to 30 cm from the mounting location of the parts to be inspected. For example, during the inspection of the vehicle it is necessary to check the seat belts are attached to the inner sill, but it is also necessary to check the condition of the outer sill (or its reinforcements if the outer sill is made of plastic cover), door pillar, floor panels or any other structural element within 30 cm from the seat belt mounting point.

## 4. ANALYSIS OF THE IMPACT OF CORROSION TO THE VEHICLE CHASSIS

A chassis of a motor vehicle is a load bearing part which can be considered as the "backbone" of each vehicle. It should be strong enough to bear any type of load, regardless of the difficult operating conditions (fully loaded vehicle or empty vehicle). The chassis (frame) consists of two longitudinal girders and several transverse connecting girders. Some types of frames have cut-outs in various shapes primarily for weight reduction. The typical materials from which the chassis are built are various types of alloy steels. Chassis parts are most often made from I, C or U profiles. During design process of the vehicle, based on the assumed and experimental values of static and dynamic loads, the chassis as the load bearing part should be dimensioned, taking into account a certain safety factor due to the assumption of possible weakening of the structure, potential overload and the impact of corrosion. It is assumed that the weakening of the chassis due to corrosion will violate the characteristics of the predicted factory load capacity and safety parameters of the operation that the vehicle had at the beginning of its working life.

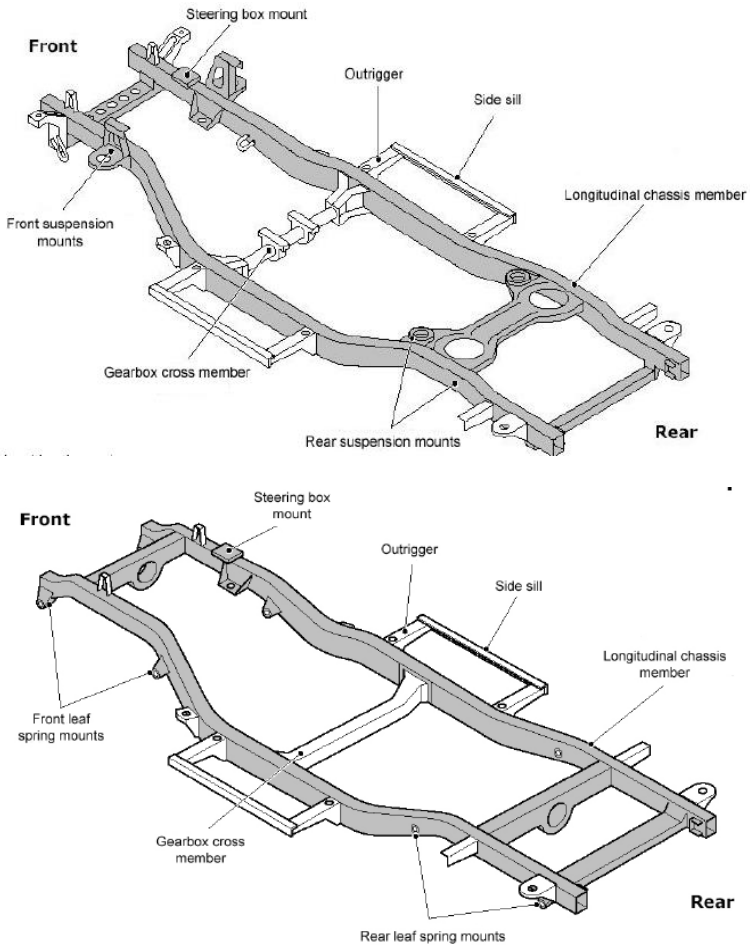


*Figure 2 The important load bearing partsof a passenger vehicle*

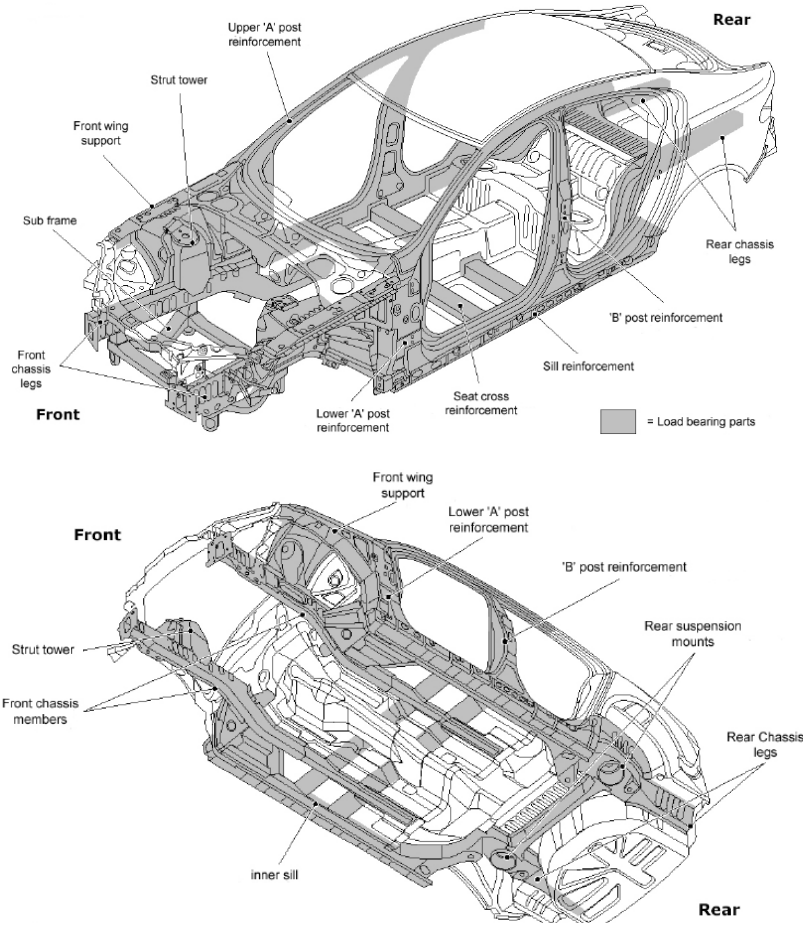


*Figure 2 Continued*

In this paper, we analyzed the influence of general corrosion to the chassis, in a way that influence of corrosion was simulated by reducing the thickness of the chassis profile [1]. We take an assumption that the corrosion is uniformly distributed, i.e. the thickness of the bearing elements decreases uniformly due to corrosion (although an unevenly distributed corrosion is the most common case in reality). Also, by reducing the thickness of the profile, some critical areas can be identified to which additional attention should be paid, both during the design process and in inspection of the chassis condition in exploitation. We used the SolidWorks simulation package for FEM analysis [9]. We analyzed the chassis for three cases of static load:

- Case I - analysis of static load of the factory designed structure (thickness of profile = 8 mm),
- Case II - analysis of the chassis of a vehicle which has been operated for 20 years (thickness of profile = 7.4 mm),
- Case III - analysis of the chassis of a vehicle which has been operated for 30 years (thickness of profile = 6.5 mm).

For all three cases of analysis, all input parameters are the same, only the profile sheet metal (longitudinal and transverse) changed its thickness due to the action of corrosion. According to the available empirical data from the literature, the degree of corrosion action is about 0.02 mm in material decrease per year. The relationship between time and material decrease is not linear. At the beginning of vehicle operation, the effect of corrosion is minimal due to good protection of the surface layer of the metal parts, but with the passing of time and the negative effects of operating conditions, the degree of protection of the chassis surface decreases and the amount of removed material increases. The effect of corrosion is especially increased if the structural element is mechanically damaged.

### *4.1 A design chassis data*

For the purposes of this analysis, the chassis of the Mercedes-Benz Actros 3344s / 33 truck was chosen. All the necessary data has been taken from the official Mercedes website and the Actros Mercedes specification (a document intended to inform potential customers) [8].

#### 4.1.1 Material properties and dimensions

The material from which the chassis is made is alloy steel DIN 1.0984, with following mechanical properties: density = 7800 kg/m$^3$, minimum yield strength ReH = 500 (MPa), tensile strength Rm = 700 (MPa), Young's modulus of elasticity = 210000 (MPa), Poisson's ratio= 0.28, shear modulus = 79000 (MPa). Figure 3 shows dimensions of the analyzed chassis.

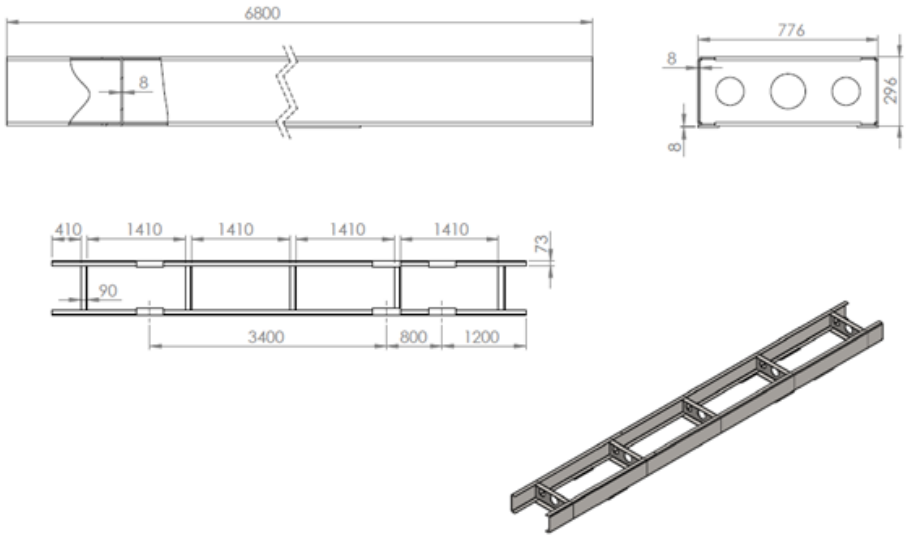


*Figure 3 Dimensions of the analyzed chassis [1]*

The load capacity of the truck is 24 t, and it is assumed that the force of gravity of the load acts in the middle of the cargo space.

#### 4.1.2 Chassis supports (same for all three cases of analysis)

The support of the chassis represents location where contact between the chassis and the truck axle is made. The chassis transmits force to the axles via the supports and further to the ground. In the analysis, slider-shaped supports were taken for 4 supports, while 2 supports were fixedly connected, Figure 4.

4.1.3 Forces acting to the chassis (same for all three cases of analysis)

The chassis is loaded by external load forces and forces due to the weight of the frame, Figure 5. Force 1 represents the weight of the load from the cargo space and the weight of the body above the rear axles. Force 2 represents the force due to the weight of the body part above the front axle. This analysis was done for the loads prescribed by the manufacturer.

4.1.4 FEM model mesh (same parameters in all three cases of analysis)

In FEM analysis, the structure was devided by 21448 elements of standard shape (equilateral triangle), with 45278 nodes.

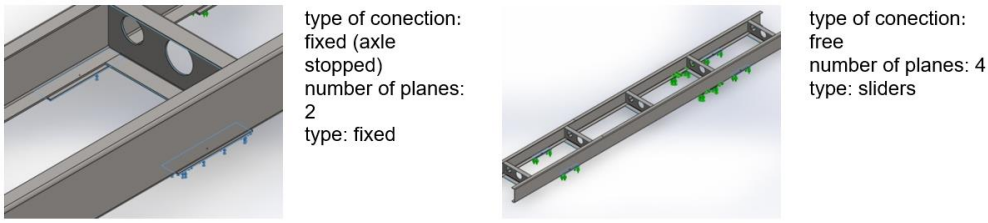


*Figure 4 Type of supports [1]*

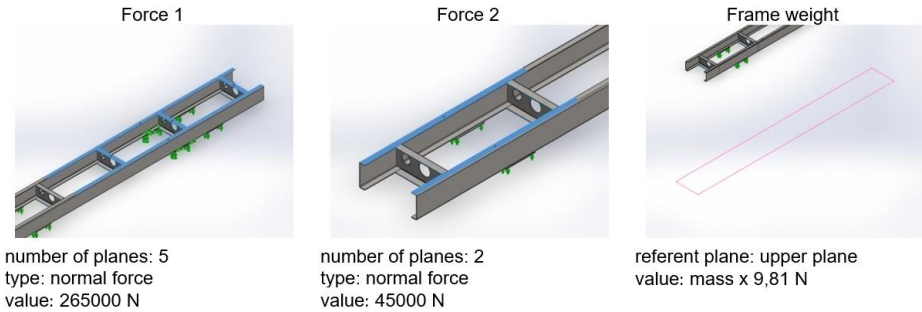


*Figure 5 Forces acting to the chassis [1]*

## 5. RESULTS OF ANALYSIS

In the FEM analysis, 4 parameters were analyzed:

- σ - stress
- μ - displacement, refers to the total displacement of nodes,
- ε - specific elongation, refers to the elongation of individual elements,
- K - safety factor, the value is calculated based on the actual stress and the allowable stress for a given material, indicating how many times the allowable stress is greater than the actual stress.

The objectives of this analysis are as follows:

- identification of critical areas of the structure,
- obtaining results which could show the extent to which corrosion has weakened the frame (change of safety factor).

The values of parameters obtained by FEM analysis are shown in Table 1, while corresponding diagrams are shown in Figures 6 – 8.

***Table 1*** *The values of analyzed parameters*

| | Thickness of long. and transv. profiles t (mm) | Max. stress σ (N/mm2) | Displacement μ (mm) | Specific elongation (for chosed surface of frame) ε | Min. safety factor K |
|---|---|---|---|---|---|
| Case I | 8,00 | 250,14 | 3,20 | 0,101 | 2,20 |
| Case II | 7,40 | 296,46 | 3,90 | 0,122 | 1,41 |
| Case III | 6,50 | 370,80 | 4,70 | 0,131 | 1,11 |

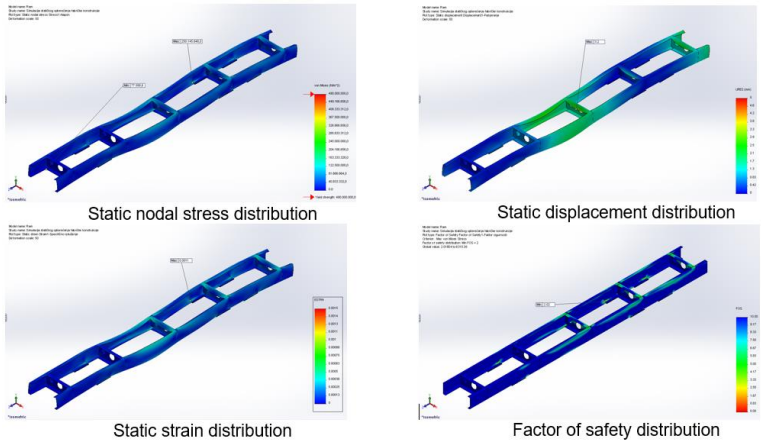


*Figure 6 Results of analysis of static load of the factory designed structure (t = 8 mm) [1]*

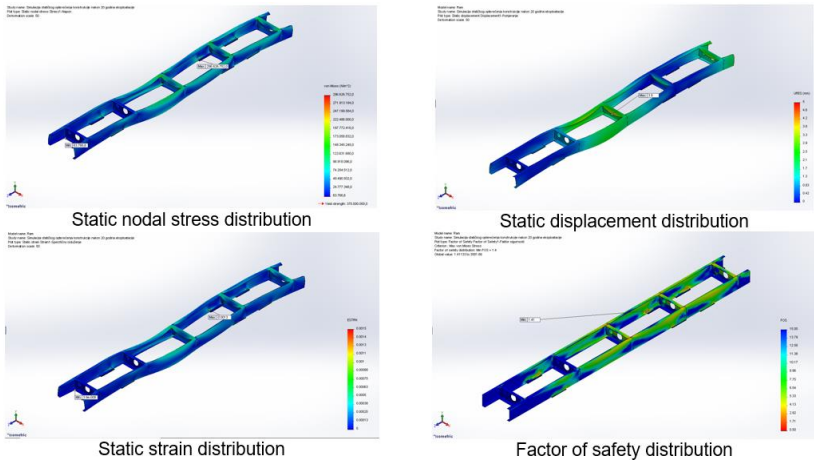


*Figure 7 Results of analysis of the chassis of a vehicle which has been operated for 20*

*years (t = 7.4 mm) [1]*

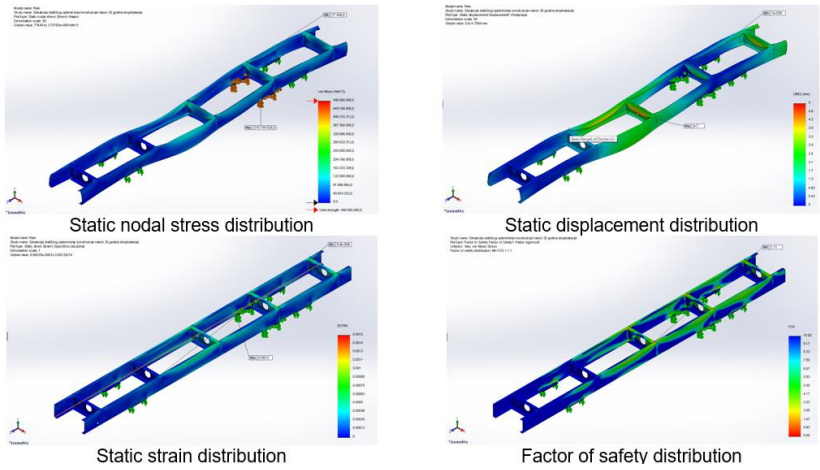


*Figure 8 Results of analysis of the chassis of a vehicle which has been operated for 30 years (t = 6.5 mm) [1]*

## 6. DISCUSSION OF RESULTS

This analysis especially emphasizes the results obtained in the form of recognized critical areas of the structure, as well as areas that are not exposed to high loads. Critical areas are those with high values of stresses, displacements, specific elongations and areas where safety factor has a minimum value. Based on the analysis, critical areas of the structure are defined as follows:

- locations where profiles are connected,
- locations of concentrated load acting,
- locations where profiles are supported (locations provided for profiles support on axles),
- intentionally weakened locations due to weight saving.

From the Figure 9, one can notice that the maximum value of the internal stress is at the location where frame is supported to the shafts. The stress value for other critical points is also close to the maximum. The minimum value of the safety factor is at the point of connection between two profiles, which are also the most loaded point due to the action of the weight of the load from the cargo space. The largest displacement occurred on the transverse profile which is also the location where the highest load acts (force 1, force 2 and weight of the frame). At this location the internal stress is close to the maximum, but not the highest. The highest specific elongation is in the lower zone of the longitudinal girders.

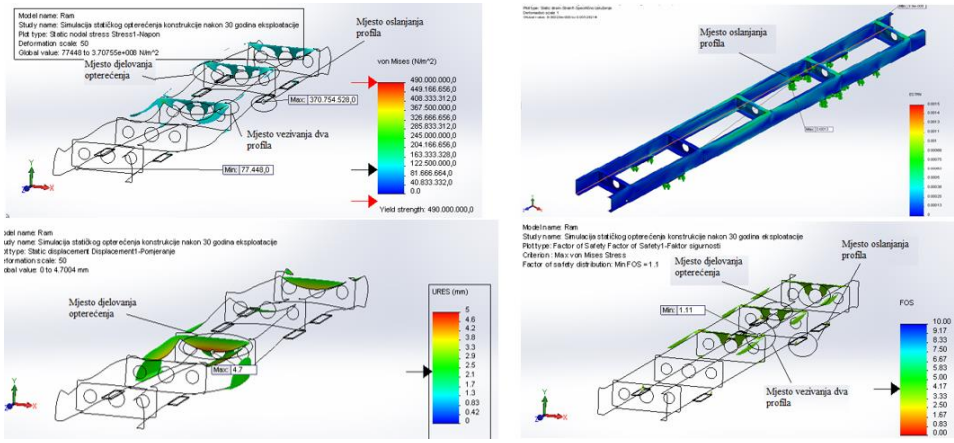


*Figure 9 Critical areas of the frame [1]*

The theoretical limit value of the safety factor during design is 1 If it happens that the safety factor value decreases below 1, the frame will be probably plasticly deformed, i.e. the deformations of the frame will be permanent. According to the data given in Table 1, it is obvious that safety factor decreases as the chassis time in exploatation increase. The reduction of the safety factor was expected, and the obtained value leads to the conclusion that the assumption that corrosion has a negative effect to the vehicle frame was correct.

## 7. CONCLUSIONS

Corrosion that occurs on vehicles is a problem that endangers traffic safety, and its negative financial effect is also significant. Corrosion that has occurred on important load-bearing parts of the vehicle reduces their designed strength and rigidity, i.e. the ability to carry the projected load, and thus directly affects the safety of vehicles in traffic. A recognition of critical locations are important for any structure. It is especially important to emphasize that critical locations from the point of view of load are often critical locations from the aspect of corrosion action. Thus, for example, due to the connections between profiles (welds, rivets, wedges, screws), regardless of the fact that the profiles are made of the same material, the corrosion may happened (due to the gaps in which moisture remains, as well as salt). Also, the locations where profile are deformed and locations where material is cut-off due to weight saving are suitable for corrosion action due to the potential poor surface protection or possible mechanical damage. The locations where concentrated loads act are the points of support of the cargo box, the points of support of the cabin, etc. In order to eliminate the effect of corrosion, most manufacturers significantly strengthen the structur's dimensions. According to the data which can be found in literature, the value of the safety factor in design process can be from 3 to 40. So, overdesign is the way to ensure the structure will be safe, as well its environment. However, the structure can break and fail due to improper operation (overloading), inadequate maintenance, as well as insufficient control of the condition of the vehicle. Therefore, during periodic inspections of vehicles, it is important to determine the condition of the vehicle in terms of corrosion and structural integrity, especially the load-bearing structural elements on which other parts of the vehicle are placed.

**REFERENCES**

[1] Aleksić, M.: "Corrosion of load bearing structures of motor vehicles", bachelor thesis, Faculty of Mechanical Engineering Banja Luka, 2016.

[2] Fujita, S., Kajiyama, H., Kato, C.: "Assessment and Application Technologies for Automotive Materials (Perforation) —Techniques for Corrosion Resistance and Perforation Feedback for Automotive Steel Materials", JFE technical report, 2004, No. 4, pp. 9-16.

[3] Golubović-Bugarski, V., Globočki Lakić, G., Petković, S.: "Corrosinon and structural integrity of vehicles", Profesional Conference Technical inspection of vehicles of Republika Srpska, (organised by University of Banja Luka, Faculty of Mechanical Engineering), 2015.

[4] Johnson, J.T.: "Corrosion Control and Prevention - Appendix N - Motor vehicles", The Body Division of the Automotive Corrosion and Prevention Committee of the Society of Automotive Engineers, 2000.

[5] Koch, G.H., Brongers M.P.H., Thompson N. G.: "Corrosion Costs and Preventive Strategies in the United States", The U.S. Federal Highway Administration, publication no. FHWA-RD-01-156, NACE International, 2002.

[6] MOT Inspection Manual, "Appendix C: Structural integryti and corrosion", 2011, Vehicle and Operator Services Agency.

[7] Wikipedia, available at: https://en.wikipedia.org/wiki/corrosion, Accessed: 10.09.2020.

[8] Mercedes-benz, available at: https://www.mercedes-benz.com/, Accessed: 10.09.2020.

[9] SOLIDWORKS, available at: https://www.solidworks.com, Accessed: 10.09.2020.

MVM – International Journal for Vehicle Mechanics, Engines and Transportation Systems

# NOTIFICATION TO AUTHORS

The Journal MVM publishes original papers which have not been previously published in other journals. This is responsibility of the author. The authors agree that the copyright for their article is transferred to the publisher when the article is accepted for publication.

The language of the Journal is English.

Journal ***Mobility & Vehicles Mechanics*** is at the SSCI list.

All submitted manuscripts will be reviewed. Entire correspondence will be performed with the first-named author.

Authors will be notified of acceptance of their manuscripts, if their manuscripts are adopted.

## *INSTRUCTIONS TO AUTHORS AS REGARDS THE TECHNICAL ARRANGEMENTS OF MANUSCRIPTS*:

**Abstract** is a separate Word document, "*First author family name_ABSTRACT.doc*". Native authors should write the abstract in both languages (Serbian and English). The abstracts of foreign authors will be translated in Serbian.

This document should include the following: 1) author's name, affiliation and title, the first named author's address and e-mail – for correspondence, 2) working title of the paper, 3) abstract containing no more then 100 words, 4) abstract containing no more than 5 key words.

**The manuscript** is the separate file, „*First author family name_Paper.doc*" which includes appendices and figures involved within the text. At the end of the paper, a reference list and eventual acknowledgements should be given. References to published literature should be quoted in the text brackets and grouped together at the end of the paper in numerical order.

Paper size: Max 16 pages of B5 format, excluding abstract
Text processor: Microsoft Word
Margins: left/right: mirror margin, inside: 2.5 cm, outside: 2 cm, top: 2.5 cm, bottom: 2 cm
Font: Times New Roman, 10 pt
Paper title: Uppercase, bold, 11 pt
Chapter title: Uppercase, bold, 10 pt
Subchapter title: Lowercase, bold, 10 pt
Table and chart width: max 125 mm
Figure and table title: Figure _ (Table _): Times New Roman, italic 10 pt

Manuscript submission: application should be sent to the following e-mail:

**mvm@kg.ac.rs ; lukicj@kg.ac.rs**
or posted to address of the Journal:
**University of Kragujevac – Faculty of Engineering**
**International Journal M V M**
**Sestre Janjić 6, 34000 Kragujevac, Serbia**

The Journal editorial board will send to the first-named author a copy of the Journal offprint.

MVM – International Journal for Vehicle Mechanics, Engines and Transportation Systems

## OBAVEŠTENJE AUTORIMA

Časopis MVM objavljuje orginalne radove koji nisu prethodno objavljivani u drugim časopisima, što je odgovornost autora. Za rad koji je prihvaćen za štampu, prava umnožavanja pripadaju izdavaču.

Časopis se izdaje na engleskom jeziku.

Časopis ***Mobility & Vehicles Mechanics*** se nalazi na SSCI listi.

Svi prispeli radovi se recenziraju. Sva komunikacija se obavlja sa prvim autorom.

## *UPUTSTVO AUTORIMA ZA TEHNIČKU PRIPREMU RADOVA*

**Rezime** je poseban Word dokument, "*First author family name_ABSTRACT.doc*". Za domaće autore je dvojezičan (srpski i engleski). Inostranim autorima rezime se prevodi na srpski jezik. Ovaj dokument treba da sadrži: 1) ime autora, zanimanje i zvanje, adresu prvog autora preko koje se obavlja sva potrebna korespondencija; 2) naslov rada; 3) kratak sažetak, do 100 reči, 4) do 5 ključnih reči.

**Rad** je poseban fajl, „*First author family name_Paper.doc*" koji sadrži priloge i slike uključene u tekst. Na kraju rada nalazi se spisak literature i eventualno zahvalnost. Numeraciju korišćenih referenci treba navesti u srednjim zagradama i grupisati ih na kraju rada po rastućem redosledu.

Dužina rada: Najviše 16 stranica B5 formata, ne uključujući rezime
Tekst procesor: Microsoft Word
Margine: levo/desno: mirror margine; unurašnja: 2.5 cm; spoljna: 2 cm, gore: 2.5 cm, dole: 2 cm
Font: Times New Roman, 10 pt
Naslov rada: Velika slova, bold, 11 pt
Naslov poglavlja: Velika slova, bold, 10 pt
Naslov potpoglavlja: Mala slova, bold, 10 pt
Širina tabela,dijagrama: max 125 mm
Nazivi slika, tabela: Figure __ (Table _): Times New Roman, italic 10 pt

Dostavljanje rada elektronski na E-mail: **mvm@kg.ac.rs ; lukicj@kg.ac.rs**

ili poštom na adresu Časopisa
**Redakcija časopisa M V M**
**Fakultet inženjerskih nauka**
**Sestre Janjić 6, 34000 Kragujevac, Srbija**

Po objavljivanju rada, Redakcija časopisa šalje prvom autoru jedan primerak časopisa.

**MVM** *Editorial Board*
*University of Kragujevac*
*Faculty of Engineering*
*Sestre Janjić 6, 34000 Kragujevac, Serbia*
*Tel.: +381/34/335990; Fax: + 381/34/333192*
***www.mvm.fink.rs***